MODELING AND CONTROL OF MULTI-AGENT SYSTEMS

A Thesis

by

MIAOMIAO ZHAO

Submitted to the Office of Graduate and Professional Studies of
Texas A&M University
in partial fulfillment of the requirements for the degree of

MASTER OF SCIENCE

Chair of Committee,	Shankar P. Bhattacharyya
Committee Members,	Aaron Ames
	Aniruddha Datta
	Erchin Serpedin
Head of Department,	Miroslav M. Begovic

Major Subject: Electrical Engineering

May 2015

ABSTRACT

Biology has brought much enlightenment to the development of human technology, for example, the collective behaviors inspired engineering applications (such as, the unmanned vehicle formation, the satellite alignment etc.), and even the study of network theory. This discipline has made a significant contribution to technology development. As a prospective solution to the current issues, multi-agent control has become a popular research topic in recent decades. The traditional control methods based on the classical models are suffering from high sensitivity to model accuracy, computational complexity, low fault tolerance, and weakness in real-time performance. Therefore, the advantages of multi-agent control are obvious: 1) easy maintenance and expansion of the system by repairing, replacing or adding agents; 2) high fault tolerance and robustness, ability to function properly even when some agents fail; 3) low requirement of distributed controllers, which brings low cost and large flexibility.

In this thesis, I investigate problems on modeling and control of multi-agent systems. In particular, I propose a three-dimensional model to simulate collective behavior under high-speed conditions. I design an improved adaptive-velocity strategy and weighted strategy to enhance the performance of the multi-agent system. Moreover, I analyze the performance from the aspects of energy and parameter space. I show how the model works and its advantages compared to existing models.

Then, I study the design of distributed controllers for multi-agent systems. Output regulation with input saturation and nonlinear flocking problems are studied with the assumption of a heterogeneous switching topology. The output regulation problem is solved via low gain state feedback and its validity verified by theoretical

study. Then, the flocking problem with heterogeneous nonlinear dynamics is solved. A connectivity-preserving algorithm and potential function are designed to ensure the controllability of the multi-agent system through the dynamic process.

Overall, this thesis provides examples of how to analyze and manipulate multi-agent systems. It offers promising solutions to solve physical multi-agent modeling and control problems and provides ideas for bio-inspired engineering and artificial intelligent control for multi-agent systems.

Dedicated to my parents - Zhaoqin Tang and Tianwu Zhao

ACKNOWLEDGEMENTS

I sincerely thank my advisor, Prof. Shankar P. Bhattacharyya. He is a mentor, like a beacon in my life, not only guides me on research, but also influences me in the way of thinking and continuously encourages me to pursue my dream with a constant positive attitude.

I also thank my thesis committee members Profs. Aaron Ames, Aniruddha Datta, and Erchin Serpedin. I am proud to be part of the control group advised by Prof. Bhattacharyya. I thank group members for fun memories and valuable research feedback, including Narayani Vedam, Zhangxin Zhou, Ivan de Jesus Diaz Rodriguez, Navid Mohsenizadeh, and Dr. Wei Zhang. I thank my undergraduate advisor and teammate, Housheng Su and Miaomiao Wang, thanks for their continuous guide and cooperation. Dr. Su and Miaomiao Wang led me to the exploration of multi-agent systems.

My graduate student life would not be so colorful and interesting without all my lovely friends: Ruixian Liao, Yao Luo, Jingqing Wang, Zhangxin Zhou, Tingshan Yu, Xi Liu, and Jiayuan Zhang.

Finally, I am so fortunate to have been born and raised in the most supportive family. My parents' love and support make me feel like I am at home even when I am physically on the other side of the earth.

TABLE OF CONTENTS

Page

LIST OF FIGURES

LIST OF TABLES

TABLE Page

1. INTRODUCTION

In nature, biological systems display diverse group behaviors via simple rules and interactions between the individuals in the group such as bird flocking, fish schooling, bacterial colony formation, insect swarming, etc as shown in Figure 1.1 [1–4]. Research on multi-agent systems can be roughly divided into three categories [5]: behavioral patterns summarized from observations of biological phenomena; mathematical modeling and simulation; control methods to manipulate artificial (or man-made) multi-agent systems.

Figure 1.1: Examples of multi-agent systems: fish schooling and bird flocking.

1.1 Thesis Objectives

In this thesis, problems in mathematical modeling and control of multi-agent systems are considered as shown in Figure 1.2. Specifically, the problems in this thesis can be divided into four main parts.

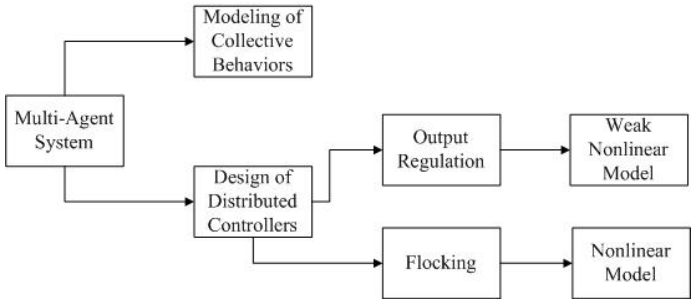

Figure 1.2: Summary of the research topics in this thesis.

1.1.1 Modeling of Three-Dimensional Collective Behavior

There are many papers devoted to building collective behavioral models with simple decision-making rules [6–9]. Reynolds developed a fundamental model named Boid in 1987 with three simple rules as shown in Figure 1.3 [7]: collision avoidance, velocity matching, flock centering. In 1995, Vicsek et al. simplified the Boid model [8], and established that the randomly initialized system achieves velocity synchronization and position stabilization when the group density is high and measurement noise is small. In 2002, Couzin et al. extended the Vicsek model to three-dimensional space with more biological features such as three sensing zones and so on, named the Couzin model [9] shown in Figure 1.4. The Couzin model exhibits unusual behaviors such as torus and highly parallel as shown in Figure 1.5.

The Boid, Vicsek, and Couzin models can emerge collective behaviors through simple interacting rules. Since then, many studies have been conducted on the Vicsek model and the Couzin model in the literature. Most models assume that flocking agents keep a uniform and invariable speed for simplification. However, considering that agents speeds are more likely to be varying with the environment, adaptive strategies were investigated in some works [10, 11]. The idea of the adapting of the velocity leads to high efficiency and to improve high-speed performance. However,

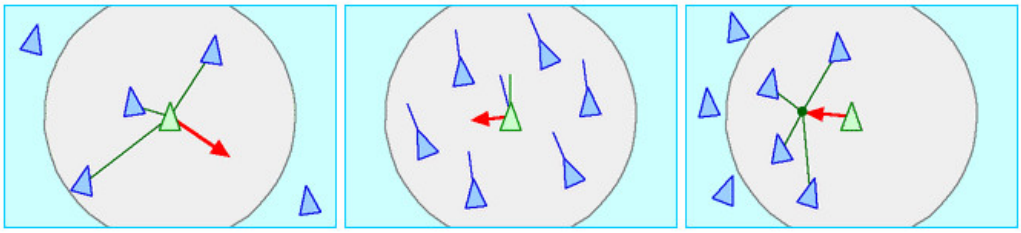

Figure 1.3: Boid model: a) collision avoidance: turn to avoid collision with neighbors; b) velocity matching: turn to the average direction of neighbors; c) position aggregation: turn to the average position of neighbors.

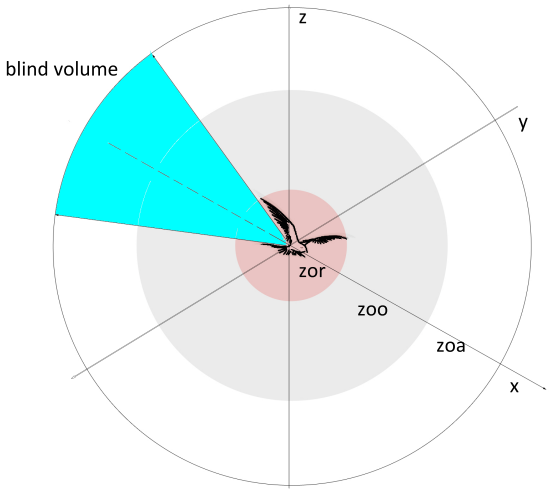

Figure 1.4: Three-dimensional collective behavior model, with considerations of blind volume and three sensing zones: zone of repulsion, zone of orientation, and zone of attraction. Details are included in Section 3.1.2.

in current research, the degree of adaptation is preset and invariable throughout the dynamic process. Moreover, due to the neglect of information from agents themselves, the adaption fails under some certain circumstances. Furthermore, numerical experiments have revealed a trade-off between the improvement of high-speed performance and fast convergence with a preset adaptive degree. In view of the above, it is necessary to design a new interacting rule to increase the running speed, and at

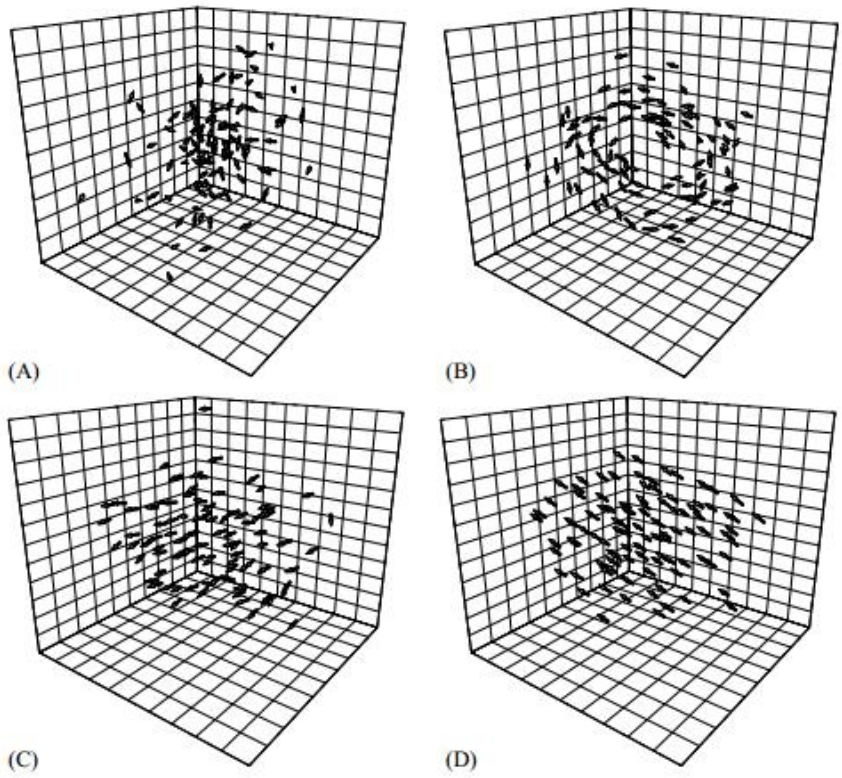

Figure 1.5: Types of behaviors in the Couzin model: (A) initial random state; (B) torus; (C) dynamically parallel; (D) highly parallel.

the same time, maintain good convergence, as well as avoid the failure of adaptation and to improve the trade-off. Moreover, small revisions of the adaptive strategy are preferred to preserve the simplicity of the model.

In addition, research on complex networks [12, 13] demonstrates that in most communication networks, nodes have different degrees of connectivity with their neighbors. A node with a larger degree have greater influence on the structure and dynamics of the network. Existing research on the Vicsek model [12] has revealed that the weighted strategy can enhance convergence efficiency. Instead of one sensing zone in the Vicsek model, the Couzin model has three sensing zones: the zone of

repulsion (zor), the zone of orientation (zoo), and the zone of attraction (zoa). To ensure quick convergence, the orientational effect should be amplified, it is reasonable to design a new strategy to assign weights.

In summary, the adaptive-velocity and the weighted strategies not only enhance the system performance in high-speed conditions and allow more realistic considerations, but also maintain the simplicity of the collective model. In this thesis, new strategies are designed based on these principles. They inherit the advantages of the existing ones and avoid their invalid conditions. A new model with the new strategies is carried out and analyzed with regard to both high-speed performance and convergent speed.

1.1.2 Nonlinear Flocking Problem

Boid is a classical flocking model as shown in Figure 1.3. Most previous works on flocking control focus on linear systems especially systems with double-integrator dynamics [27,28]. However, in reality, autonomous agents might be governed by more complicated nonlinear dynamics. In fact, in synchronization of complex dynamical networks [13], nonlinear dynamics is commonly used. Consensus and flocking of multi-agent systems with some uniform nonlinear dynamics were investigated in [29]. Many theoretical studies on flocking of multi-agent systems tracking a (virtual) leader focus on linear systems and/or networks with a fixed-coupling topology and uniform intrinsic agent dynamics. Then, design of a feasible control method for a multi-agent flocking system with heterogeneous nonlinear intrinsic dynamics can relax the constraints of this problem.

1.2 Specific Contributions

In this thesis, I make original contributions in the areas of algorithms and theories of multi-agent systems. More specifically, the contributions of this thesis are as

follows:

1) In the first part, I propose an improved adaptive-velocity self-organizing model as a prospective candidate in order to enhance high-speed convergence and accelerate convergence. Moreover, a new way to assign weights is proposed to reinforce convergence under super high-speed circumstances.

2) To the best of my knowledge, input saturation has not been taken into account in the output regulation problem of general dynamic agents. I solve this problem via low gain feedback such that the tracking error can be eliminated with bounded control inputs.

3) I investigate the multi-agent flocking problem with heterogeneous nonlinear dynamics. I construct a potential function and a connectivity-preserving flocking algorithm to ensure the agents stay connected. The assumption is mild that the initial network is connected, and the coupling strength of the initial network of the nonlinear velocity consensus term is greater than a certain threshold.

1.3 Thesis Organization

At the beginning of this thesis, the background of current research on multi-agent systems and the importance of this topic will be presented. Then, we will discuss two subtopics in multi-agent systems: modeling via behavioral rules and distributed control law design as shown in Figure 1.2. A new model is built in the first part to mimic collective behavior in nature. In the second part, control approaches are proposed to solve weakly nonlinear, and general nonlinear multi-agent control problems. Summary and future research will be presented in the last chapter.

2. LITERATURE RESEARCH ON MODELING AND CONTROL OF MULTI-AGENT SYSTEMS

Recent years have witnessed an increasing research interest in the coordination of multi-agent systems because of its extensive applications to biological, social and engineering systems, such as animal groups, economic behaviors, sensor networks, space crafts, unmanned aerial vehicles (UAVs), mobile robots, formation and attitude control, among others [6, 21, 30].

This chapter presents an overview of the background research on multi-agent systems, about how the idea of multi-agent system developed, how the behavioral and mathematical models of multi-agent systems were built. Specifically, research on multi-agent systems started from the observation of collective behaviors in nature. In this behavior, local sensing and reaction of each individual result in complex nonlinear phenomena. That is why sometimes we call this behavior 'collective intelligence'. Mammal herds, bird flocks, and fish schools are examples of collective intelligence. Even simple organisms such as bacteria can form a precisely symmetrical colony. This emergence also enlightens human beings. On one hand, people are working on the improvement of a single device to be more precise, efficient, and intelligent. On the other hand, collective intelligence leads to a larger probability to have a 'leap' based on the current technology. As a branch of multi-agent research, study on complex networks reveal the exponential amplification of tiny changes at the individual level, but sometimes they are able to maintain robustness [13]. In other words, if the mechanism in collective intelligence are fully studied, we can manipulate the system at very little cost and high efficiency. The relationship between these research branches is shown as Figure 2.1.

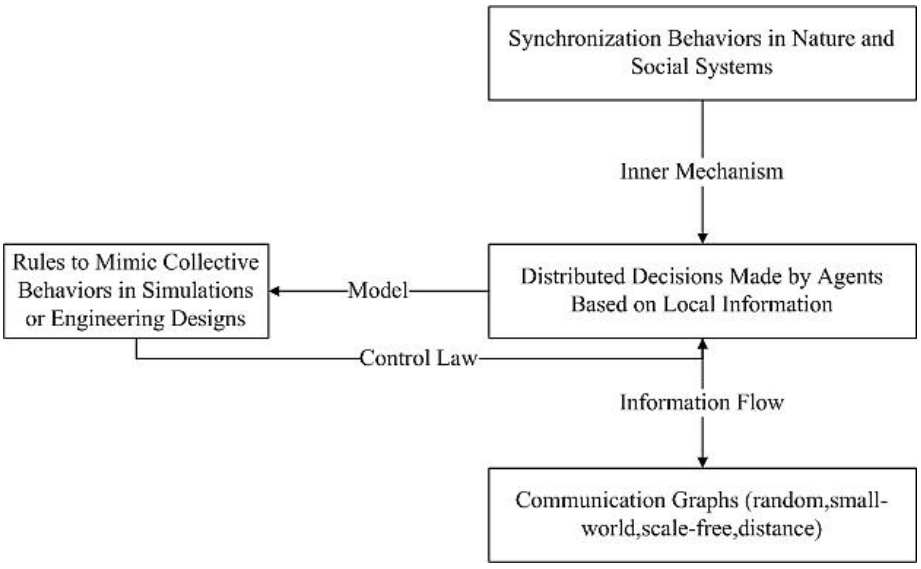

Figure 2.1: The relationship between different branches of multi-agent research

The organization of this chapter is as follows. Firstly, modeling of multi-agent systems based on behavioral rules will be introduced to simulate collective behavior in nature. Then, mathematical models based on differential equations will be presented. Networks of information flow are described in the last part of this chapter.

2.1 Behavioral Models of Collective Behavior

The collective behavior of creatures are among the most beautiful sights. The collective behaviors allow the group to achieve the objectives such as defense against predators, foraging for food which the individual can hardly achieve. In migrating bird flocks, the formation reduces the energy of individuals in flying. Mammals usually aggregate to defend predators or pursue preys. Such behavior has also been observed in human crowd panic and mob situations.

To produce collective behaviors in computer animation, a multi-agent system should be modeled. In the current literature, the most popular methods to build models of multi-agent systems are the Lagrange method [31–33], the Euler method [34,35],

and a method based on discrete behavioral rules [7–12]. The idea of Lagrange method describes the continuous motion of agents by ordinary differential equations. But by the Euler method, the multi-agent system is built as a density field described by partial differential equations. Modeling by discrete behavioral rules is computationally efficient, and easy to implement on a computer and avoid the complexity to translate linguistic rules to mathematical equations. A most important feature of multi-agent systems is that complex nonlinear behaviors can emerge from simple local interacting rules. In this section, the most basic and universal model in collective behaviors is introduced by presenting the local interacting rules [7].

2.1.1 Reynolds' Rules

Individuals in large groups are always aware of the motions of their neighbors instead of that of the whole group. Individual motion in a group is the balance of two opposite behaviors: one is a desire to stay close to the neighbors to keep aggregation; another is to a desire to avoid collisions with neighbors. Reyolds summarized the tendencies by three rules shown in Figure. 2.2.

Reynolds' Rules [7]:

1. Collision Avoidance: turn to avoid collision with neighbors;
2. Velocity Matching: turn to the average direction of neighbors;
3. Position Aggregation: turn to the average position of neighbors.

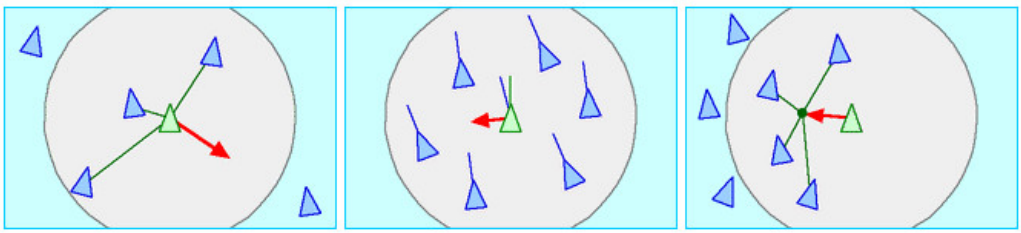

Figure 2.2: a) Collision avoidance; b) Velocity matching; c) Flocking centering.

2.1.2 Types of Communication Graphs

The communication graphs concerned in multi-agent research can be divided by three perspectives: Is the information flow symmetric at the two ends of an edge? Do the edges have weights or only take 0-1 values? Is the topology varying with time? The branches are shown in Figure. 2.3.

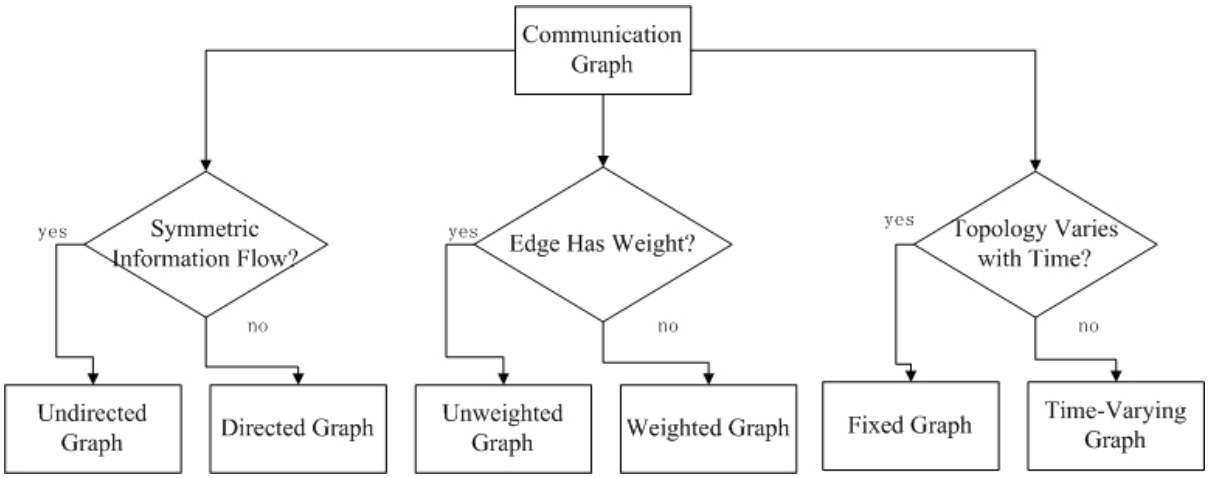

Figure 2.3: The types of communication graphs

2.2 Multi-Agent System Dynamics

Reynolds' rules summarize collective behavior very well. It can be used to design or control man-made systems. These rules rely on the information of neighbors for each individual. Thus, information flow in the communication network between agents in a group is one of the essential factors for the collective behavior. The communication network is modeled as a graph. As introduced in 2.1.2, there are different types of graphs. Here in this thesis, undirected switching topology is widely assumed. Therefore, the mathematical description of undirected switching topology

will be presented in the following as an example.

2.2.1 Mathematical Description of Communication Network

Basic concepts and results on graph theory, which are commonly used in the analysis and control of multi-agent systems, will be recalled in this section. More details could be found in [36].

$G = \{V, E, A\}$ is an undirected graph, where $V = \{v_1, v_2, ..., v_n\}$ is the vertex set and $E = \{e_{ij}\} = \{(v_i, v_j), i, j \in V\} \subset V \times V$ is the edge set. $A = \{a_{ij}\}$ is a weighted adjacency matrix defined by $a_{ii} = 0$, $a_{ij} = a_{ji} > 0$ when $\{i \neq j\}\&\{e_{ij} \in E\}$, otherwise $a_{ij} = 0$. If $a_{ij} > 0$, agent i and agent j are mutual neighbors. Therefore, the set of neighbors of agent i correspond to $\Gamma_i = \{j \in V : a_{ij} > 0\}$. $D = diag(deg(1), deg(2), \ldots, deg(n))$ is the diagonal degree matrix where $deg(i) = \sum_{j=1}^{n} a_{ij}$.

Define the Laplacian matrix $L = \{l_{ij}\}$ as $L = D - A$.

$$l_{ij} = \begin{cases} -a_{ij}, j \in \Gamma_i \\ |deg(i)|, j = i \\ 0, otherwise \end{cases} \tag{2.1}$$

An undirected graph G is said to be connected if and only if $\text{rank}(L) = n - 1$.

Lemma 1 [14]: *For an undirected graph G with L being its Laplacian matrix:*

1. L is symmetric and positive semidefinite with every row sum always being 0;

2. If G is connected, $\lambda_1 = 0$ is the only zero eigenvalue of L and $Null(L) = span[1, 1, \cdots, 1]^T$.

For a directed graph, the properties of the Laplacian matrix in Lemma 1 still hold except symmetry.

2.2.2 Dynamical Systems with Reynolds' Rules

To implement Reynolds' rules in dynamical systems control [37], define a circle with radius ρ_c which is the avoidance area of each agent. Define a collision neighborhood for agent i as $N_i^c = \{j : r_{ij} \leq \rho_c\}$ where the distance between nodes i and j is

$$r_{ij} = \|x_j - x_i\|_2 \tag{2.2}$$

Define a matching radius $\rho > \rho_c$ and the matching neighborhood by $N_i = \{j : r_{ij} \leq \rho\}$.

Then, the dynamics in two-dimensional space is:

$$\dot{x}_i = u_i \tag{2.3}$$

where $x_i = [p_i, q_i]^T \in R^2$, $u_i = [u_{pi}, u_{qi}]^T \in R^2$.

1. Collision avoidance:

$$u_i = -\sum_{j \in N_i^c} c_{ij}(x_j - x_i) \tag{2.4}$$

This control input forces agent i to turn away from neighbors within its collision radius ρ_c. c_{ij} is called the collision-avoidance gain.

2. Flock centering:

$$u_i = \sum_{j \in N_i \cap j \notin N_i^c} a_{ij}(x_j - x_i) \tag{2.5}$$

This control input pushes agent i to turn toward neighbors inside the circle with radius ρ but outside of the circle with ρ_c. a_{ij} is the flock-centering gain.

By adjusting the gains c_{ij} and a_{ij}, the influence (or preference) of collision avoidance and flock centering could be adjusted accordingly.

Alternatively, the dynamical system can be constructed as a second-order system by using the Newton's law:

$$\begin{aligned} \dot{x}_i &= v_i \\ \dot{v}_i &= u_i \end{aligned} \tag{2.6}$$

where $x_i \in R^n$ is the vector position, $v_i \in R^n$ is the velocity, and $u_i \in R^n$ is the acceleration input. This model is more realistic than Eq.2.3 physically. The distributed feedback law for this second-order system is as follows.

$$u_i = \sum_{j \in N_i} ca_{ij}[(x_j - x_i) + \gamma(v_j - v_i)] \tag{2.7}$$

where $c > 0$ is a stiffness gain, and $c\gamma > 0$ is a damping gain. Implementing the law in Eq. 2.7 can achieve both position and velocity matching. It realizes flock centering and velocity matching in Reynolds' rules. To avoid collision, the law in Eq.2.8 is introduced.

$$u_i = \sum_{j \in N_i} ca_{ij}[(x_j - x_i - \Delta ji) + \gamma(v_j - v_i)] \tag{2.8}$$

where $\Delta_{ji} \in R^n$ denotes the desired distance between agents i and j.

2.3 Multi-Agent Control Problems

From the perspective of systems control, multi-agent systems have properties such as self-adaptation, robustness and self-organization [16,19,27,38]. Roughly speaking, the control problems can be divided into several categories.

2.3.1 Consensus

The dynamic system in the consensus problem could be first-order, second-order, or higher-order. As shown in Figure 2.4, the states in the dynamic systems could be the positions, velocities, or temperatures of the agents. The objective is to drive the system states to converge to a common value which may or may not be prescribed in advance.

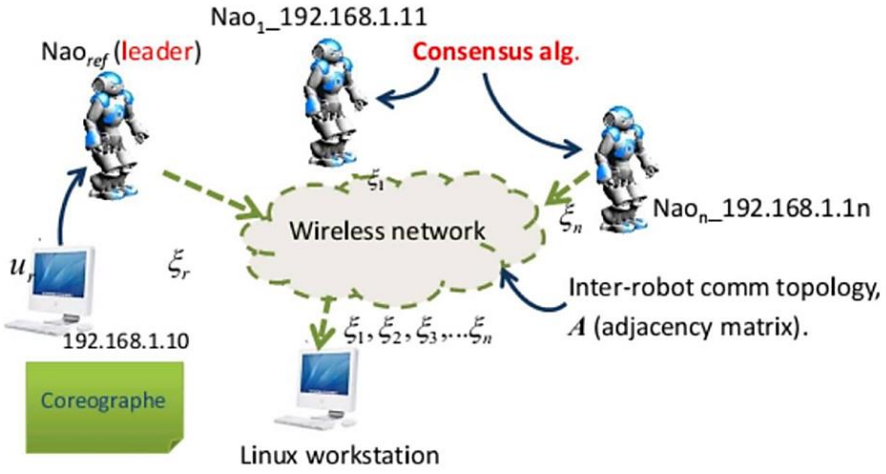

Figure 2.4: Consensus in communication networks. In this case, the information state in the consensus problem is the gestures of the robots. Information flows through wireless network.

2.3.2 Flocking

The flocking problem mainly deals with second-order systems. The states in the system are the positions and velocities of the agents. The control input has physical meaning and is the acceleration of the agents. The objective is to achieve velocity consensus, and in the meantime, the distances between agents are to be kept within desired values. The Boid model proposed by Raynold [7] is a classical example of

flocking rules as shown in Figure 2.2.

2.3.3 Swarm

The swarm problem is usually applied to first-order systems. As shown in Figure 2.5, the swarm phenomenon is the most common in nature. The objective is to maintain the positions of agents in the system in a bounded region centered at the weighted position sum.

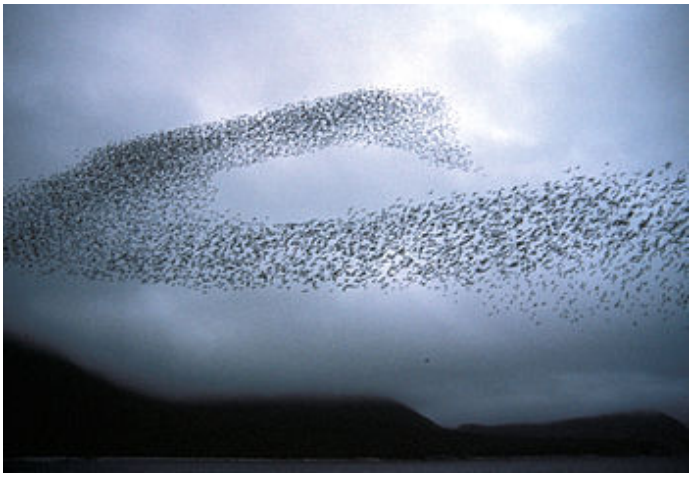

Figure 2.5: Output regulation

2.3.4 Formation

The formation problem usually deals with second-order systems. The objective is to achieve velocity consensus, and at the same time, to keep the distance between agents within desired values so that the group forms a specific shape. This problem has attracted a lot of attention because of its potential application to robots, unmanned vehicles, and computer animation [21] as shown in Figure 2.6.

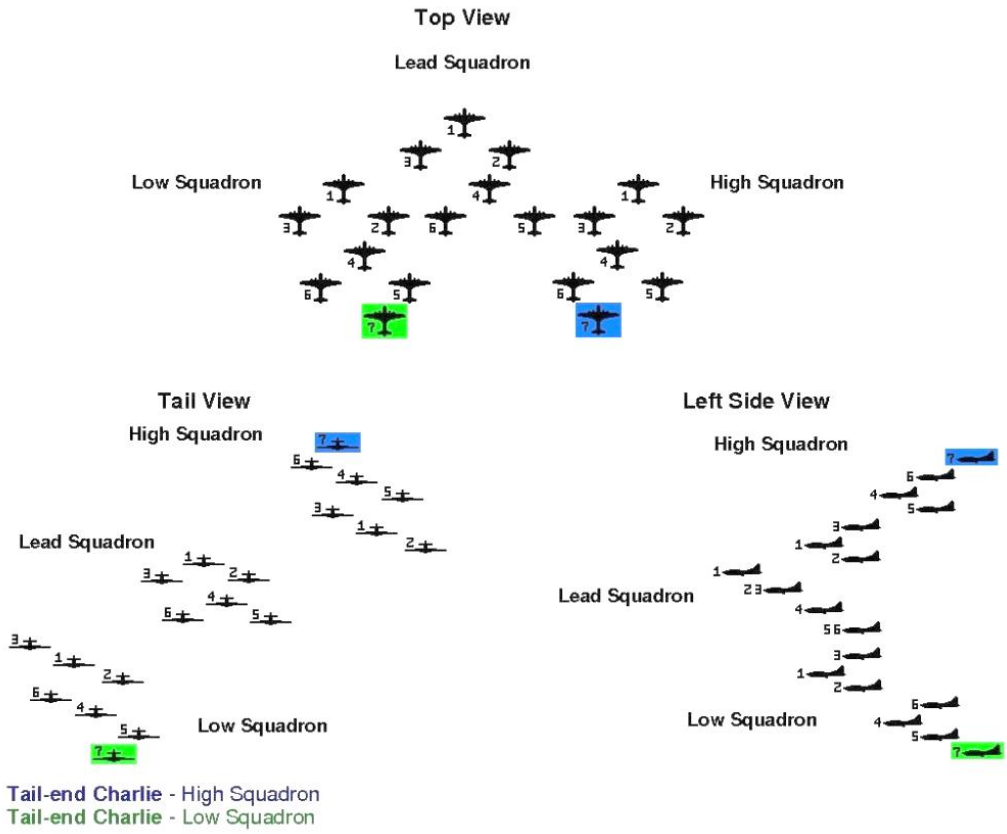

Figure 2.6: Output regulation

2.3.5 Others

Other problems such as mobile sensor networks, coupled oscillators, UAV surveillance [28, 38] are also popular research topics.

2.4 Conclusion

In this chapter, the background of multi-agent system research has been presented. As a common phenomenon existing in nature, collective behavior attracts much attention. Researchers study the mechanisms from observations and construct man-made multi-agent systems to achieve desired collective behaviors. As a typical example, Reynolds' rules have been discussed from the linguistic rules to mathemati-

cal description and control design. In the end, some classical problems on multi-agent systems were introduced.

With this background, I will introduce more behavioral models in the next chapter with more realistic consideration of reality in the next chapter and propose a novel model to improve high-speed performance. The control problems will be identified and solved in the following chapters.

3. A WEIGHTED ADAPTIVE-VELOCITY COLLECTIVE BEHAVIOR MODEL AND ITS HIGH-SPEED PERFORMANCE

This chapter proposes an improved adaptive-velocity collective behavior model as a prospective candidate in order to enhance high-speed convergence and accelerate convergence. Moreover, a way to assign weights are introduced in order to amplify orientational effect and reinforce convergence under super high-speed requirements. System performance is assessed via group polarization, convergence ratio and convergent time. By numerical experiments, super high-speed performance, convergent time, and kinetic energy will be examined in the improved adaptive-velocity model. Then, the parameter space of the weighted adaptive flocking model is investigated.

The chapter is organized as follows. Section 3.1 will present the description of two classical collective models, the Vicsek model and the Couzin model, with introduction of their properties and behaviors, respectively. With the problems raised in Section 3.1, the improved adaptive-velocity and the weighted strategies will be introduced in the next two sections. Simulation results and analysis are given in Section 3.4. Section 3.5 is the conclusion, and presents remaining issues and future work.

3.1 Two Classical Collective Behavior Models

In this section, two classical collective behavior models will be presented. The analysis of their properties reveal their advantages to simulate collective behavior. However, they also exhibit a sharp decrease with the increase of individual's speed.

3.1.1 The Vicsek Model in Two-Dimensional Space

Vicsek etc. [8] used the interaction radius r as the unit to measure distances ($r = 1$), while the time unit $\Delta t = 1$ was the time interval between two updates of

the directions and positions. In most of our simulations we used the simplest initial conditions: (i) at time $t = 0$, N particles were randomly distributed in the cell and (ii) had the same absolute velocity v and (iii) randomly distributed directions $\{\theta_i\}$. the velocities $\{v_i\}$ of the particles were determined simultaneously at each time step, and the position of the ith particle updated according to:

$$x_i(t+1) = x_i(t) + v_i(t)\Delta t \tag{3.1}$$

Here the velocity of a particle $v_i(t+1)$ was constructed to have an absolute value v and a direction given by the angle $\theta(t+1)$. This angle was obtained from the expression:

$$\theta(t+1) = < \theta(t) >_r + \Delta\theta \tag{3.2}$$

where $< \theta(t) >_r$ denotes the average direction of the velocities of particles (including particle i) being within a circle of radius r surrounding the given particle. $\Delta\theta$ is a random noise chosen with a uniform probability from the interval $[\eta/2, \eta/2]$.

The actual simulations were carried out in a square shaped cell of linear size L with periodic boundary conditions. Namely, when an agent flees away from Figure 3.1 shows the convergent process of the Vicsek model. In this figure, the velocities of the particles are displayed for varying values of the density and the noise. The actual velocity of a particle is indicated by a small arrow, while their trajectory for the last 20 time steps is shown by a short continuous curve. The number of particles is $N = 300$ in each case. (a) $t = 0$, $L = 7$, $\eta = 2.0$. (b) For small densities and noise the particles tend to form groups moving coherently in random directions, here $L = 25$, $\eta = 0.1$. (c) After some time at higher densities and noise ($L = 7$, $\eta = 2.0$) the particles move randomly with some correlation. (d) For higher density and small

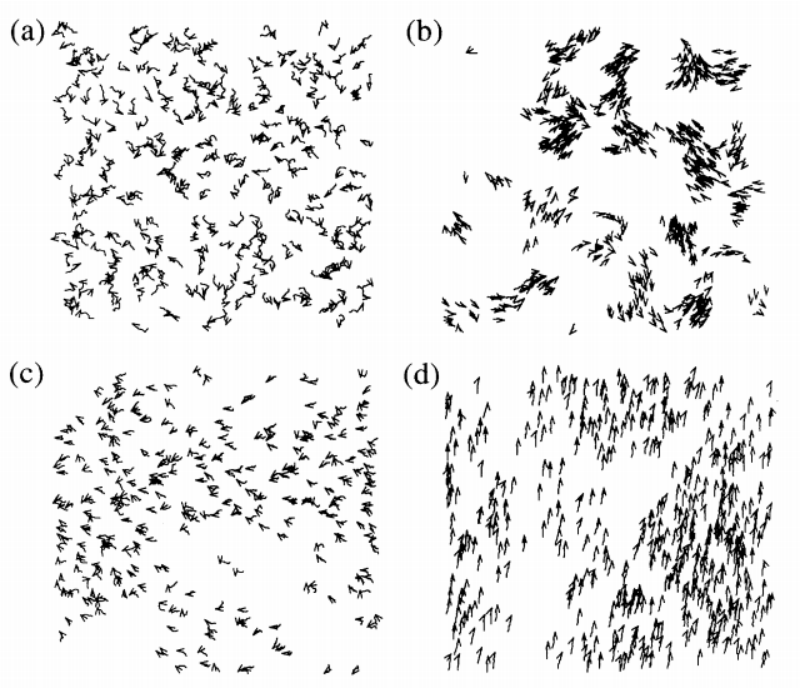

Figure 3.1: The convergent process of the Vicsek model.

noise ($L = 5$, $\eta = 0.1$) the motion becomes ordered. All of the results shown in Figure 3.1, Figure 3.2 were obtained from simulations in which v was set to be equal to 0.03.

The contribution of their work is that they concluded that the convergence is enhanced when the agent's speeds are small and the noise is small as shown in Figure 3.2. Namely, any increase of agent's speeds or noise results in divergence. From Figure 3.2, agents' speed was set to be $(0, 1]$ which is very small.

3.1.2 The Couzin Model in Three-Dimensional Space

Couzin etc. [9] use a more biologically realistic (yet still simple) model of collective behavior that is based upon an abstraction of aggregation tendencies evident in biological systems. Following the approach of Reynolds [7], he simulated the behavior of individuals as resulting from local repulsion, alignment and attractive

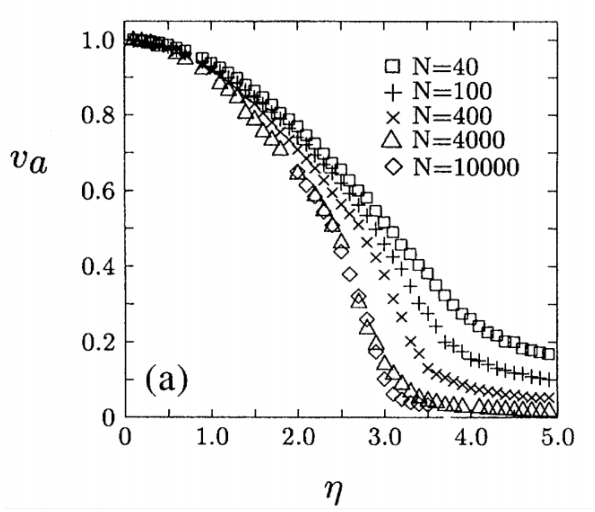

Figure 3.2: Maximum agents' speed v_a *v.s.* noise η in the Vicsek model

tendencies based upon the position and orientation of individuals relative to one another. In the Couzin model, the individual behavior results in group formation and cohesion, rather than fixing individual density within a periodic domain (as in the Vicsek model, agents will reenter the square space after they leave it from the other side). Their simulation exhibits characteristic collective behaviors, similar to those of natural groups, when certain parameters are changed.

Consider N agents, labeled from 1 through N, all moving in a continuous 3-D Euclidean space. In the Couzin model, the agents are moving at a uniform constant speed but in various directions, with initial positions and directions randomly distributed within a sphere. Shown as Figure 3.3, for each agent, the zone centered at itself can be divided into three parts, namely *zor*, *zoo*, *zoa*, respectively. The radius is divided into Δr_r, Δr_o, Δr_a, accordingly. The blind volumes and maximum turning rate are considered for every agent.

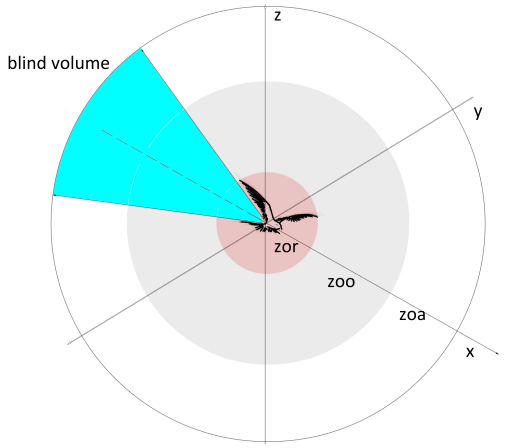

Figure 3.3: Representation of an individual in the model centered at the origin. *zor*: zone of repulsion, *zoo*: zone of orientation, *zoa*: zone of attraction. The possible blind volume behind an individual is also shown.

The Couzin model is described as follows:

$$\vec{c_i}(t+\tau) = \vec{c_i}(t) + \tau \cdot v_0 \cdot \vec{d_i}(t) \tag{3.3}$$

where $\vec{c_i}(t)$ denotes the position vector, v_0 is the value of the speed, τ denotes the time step increment, $\vec{d_i}(t)$ is the unit direction vector at step t and updates according to real-time neighborhood information, $\vec{c_i}(t+\tau)$ denotes the position in the next time step.

If there exist neighbors in *zor* of agent i,

$$\vec{d_i}(t+\tau) = -\sum_{j=1, j\neq i}^{n_{ri}} \frac{\vec{r}_{ij}(t)}{|\vec{r}_{ij}(t)|} \tag{3.4}$$

If there's no neighbor in *zor* and only exist neighbors in *zoo* of agent i,

$$\vec{d_i}(t+\tau) = \vec{d_o}(t+\tau) = \sum_{j=1, j\neq i}^{n_{oi}} \frac{\vec{v}_j(t)}{|\vec{v}_j(t)|} \tag{3.5}$$

If there's no neighbor in *zor* and only exist neighbors in *zoa* of agent i,

$$\vec{d_i}(t+\tau) = \vec{d_a}(t+\tau) = \sum_{j=1, j\neq i}^{n_{ai}} \frac{\vec{r}_{ij}(t)}{|\vec{r}_{ij}(t)|} \tag{3.6}$$

If there's no neighbor in *zor* and exist neighbors in both *zoo* and *zoa* of agent i,

$$\vec{d_i}(t+\tau) = \frac{1}{2} \cdot (\vec{d_o}(t+\tau) + \vec{d_a}(t+\tau)) \tag{3.7}$$

If there's no neighbor in *zor*, *zoo* and *zoa*,

$$\vec{d_i}(t+\tau) = \vec{v_i}(t) \tag{3.8}$$

where $\vec{r}_{ij} = (\vec{c_j} - \vec{c_i})/|(\vec{c_j} - \vec{c_j})|$ is the unit vector in the direction of neighbor j, n_{ri}, n_{oi} and n_{ai} denote the number of neighbors in *zor*, *zoo* and *zoa* of agent i, respectively.

The Couzin model has good convergence performance when each individual has a speed of $[1, 3]$ units. Some special behaviors such as torus emerges in this model as shown in Figure 3.4.

The Couzin model can exhibit different collective behaviors. Small changes on the individual level result in great changes on the group level. The model predicts that animal groups can change rapidly between these states. For instance, a group changes between the torus and dynamic parallel. Biologically, the transitions allow animal groups to vary from one type of group structure to another due to internal (e.g. hunger) or external (e.g. detection of a predator) stimuli. The tendency of individuals to align with others in the parallel group types is important not only because it minimizes distances between individuals and facilitating group movement, but also because it allows the information transportation in the group.

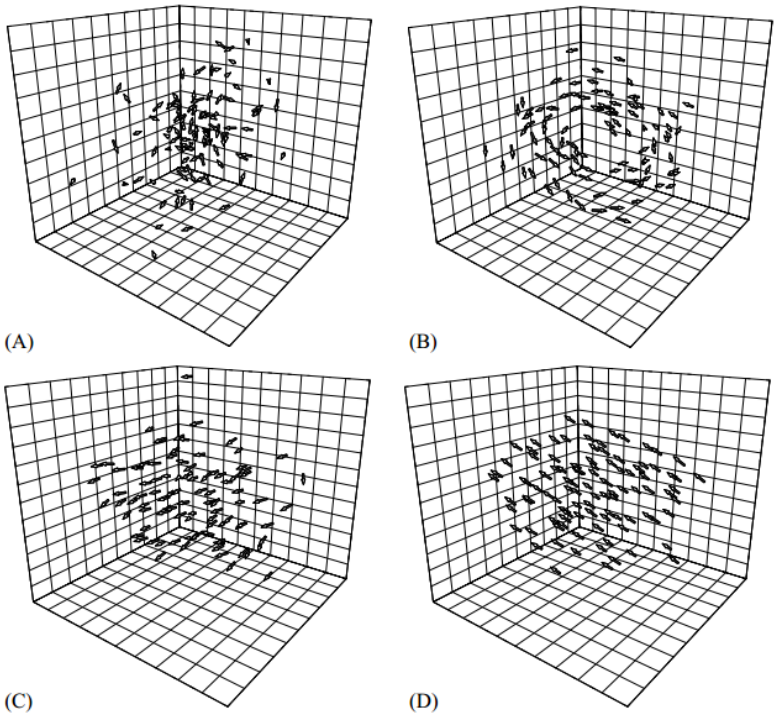

Figure 3.4: Types of behaviors in the Couzin model: (A) initial random state; (B) torus; (C) dynamically parallel; (D) highly parallel.

With the properties stated above, the Couzin model behaves satisfactorily when agents' speeds take values from $[1, 5]$. Dong etc. [11] analyzed the high-speed convergence performance and revealed that the Couzin model has the same trend as the Vicsek model: a sharp decrease of convergence performance will happen with increase of agents' speeds. The details of Dong's results will be presented in the following section.

3.2 The Improved Adaptive-Velocity Strategy

The adaptive-velocity strategy is described as follows. Agents will move at high speeds (the maximum is v_0) when their neighbors within *zoo* and themselves are

highly aligned. The improved adaptive-velocity model is given by:

$$\begin{aligned}
\vec{c}_i(t+\tau) &= \vec{c}_i(t) + \tau \cdot v_i(t) \cdot \vec{d}_i(t) \\
v_i(t) &= v_0 \cdot [u_i(t)]^{\phi} \\
u_i(t) &= \frac{1}{n_{oi}} \left| \sum_{j=1, j\neq i}^{n_{oi}} \vec{d}_j(t) \right|
\end{aligned} \tag{3.9}$$

where ϕ denotes the adaptive degree, n_{oi} denotes the number of neighbors in the *zoo* of agent i, $|\cdot|$ denotes the norm of a vector. $v_i(t)$ denotes the speed of agent i at time t, $0 \leq |v_i(t)| \leq v_0$ since $0 \leq u_i(t) \leq 1$.

To enhance the high-speed system performance, the speed adaption is designed to be influenced by both the neighborhood information and agents own directions. An adaptive ϕ is defined as follows:

$$\begin{aligned}
\phi_i(t) &= \tan \frac{\delta_i(t)}{2} \\
\delta_i(t) &= < \vec{d}_i(t), \sum_{j=1, j\neq i}^{n_{oi}} \vec{d}_j(t) >
\end{aligned} \tag{3.10}$$

where $< \cdot >$ is the angle between two vectors, $\delta_i(t) \in [0, \pi]$ denotes the angle between the direction of agent i and the average direction of its neighbors in *zoo*. Thus, for any agent i, $\phi_i(t)$ decreases with $\delta_i(t)$, namely $\phi_i(t) \to 0$ ($\phi_i(t) \to \infty$) as $\delta_i(t) \to 0$ ($\delta_i(t) \to \pi$).

In the constant-ϕ model [11], the agents' speeds are adaptive with $u_i(t)$, while the adaptive degree ϕ is a preset constant in Eq.(3.9). However, on one hand, due to the neglect of the information from the agent itself, the speed adaption will fail under some circumstances. For instance, if an agent's neighbors are highly aligned but the agent itself is moving in a direction opposite to that of its neighbors, $u_i(t)$ is large

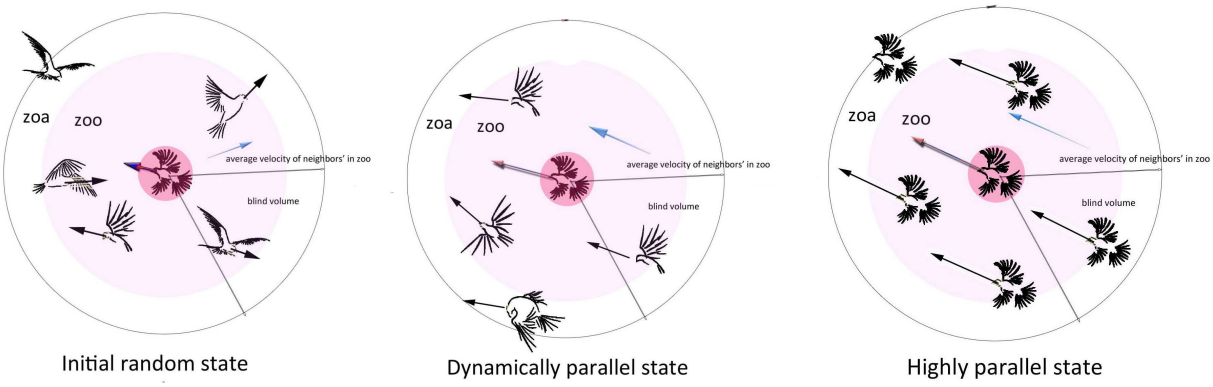

Figure 3.5: Convergent process with the improved adaptive-velocity strategy. Note that highly parallel state is deemed as convergence.

and the speed $v_i(t)$ is large. In this condition, this agent will flee away due to the lack of adaptive mechanism in this condition. Especially in high-speed conditions, a quick divergence will happen. On the other hand, when the system has achieved convergence, $u_i(t)$ is approximately equal to 1, ϕ has little influence on the value of $v_i(t)$. Therefore, a large value of ϕ is not necessary to force convergence.

Figure 3.5 shows the convergent process of the improved adaptive-velocity model in Eq.(3.10). In the initial random state, the speed of agent i significantly decreased with the adaptive parameters $u_i(t)$ and $\phi_i(t)$ and then gradually increased with alignment. This mechanism prevents quick divergence at initial random state. When the system achieves convergence, $\delta_i \approx 0$, $\phi_i \approx 0$, $|\vec{v}_i| \approx v_0$, all the agents move in the maximal speed v_0 and in a uniform direction, degenerates to the Couzin model. When the speed adaption fails in the constant-ϕ model [11], namely, when all the neighbors of an agent are highly aligned but the agent is moving in the opposite direction of its neighbors, $\phi_i(t)$ in the new adaptive model is large with $\delta_i(t) \approx \pi$, the corresponding speed $v_i(t) = v_0 \cdot [u_i(t)]^{\phi_i(t)}$ is very small which means the speed adaption is effective in this case.

3.3 The Weighted Strategy

Agents with more neighbors have greater influence on the structure and dynamic process of the system. In complex networks, the number of neighbors are defined as 'degree' [12,13,36]. To amplify the orientational effect which would speed up velocity alignment and enhance convergence performance, we propose a new way to assign weights by using the number of neighbors in *zoo*. The weighted direction iterative function is designed:

$$\begin{aligned}\vec{d}_i(t) &= \frac{\sum_{j\neq i}^{n_{oi}(t)} \gamma_j^{(\lambda)}(t)\vec{d}_j(t)}{\left\| \sum_{j\neq i}^{n_{oi}(t)} \gamma_j^{(\lambda)}(t)\vec{d}_j(t) \right\|_2} \\ \gamma_j^{(\lambda)}(t) &= \frac{[n_{oj}(t)]^\lambda}{\sum_{k\neq j}^{n_{oj}} [n_{ok}(t)]^\lambda}\end{aligned} \tag{3.11}$$

where agent j and k are the neighbors in the *zoo* of agent i and j respectively, $\gamma_j^{(\lambda)}(t)$ denotes the weight of agent j at time step t, λ denotes the weight-influence degree, $\lambda = 0$ means the network is homogeneous, $\lambda = 1$ means the weighted strategy has been applied to the model.

3.4 Simulation Results

In numerical experiments, agents are initialized in a continuous three-dimensional Euclidean space: positions are initially random within a sphere with radius 40 units; speeds are randomly generated in the range of $[0, v_0]$; directions are also randomly initialized. The consequences of varying values of parameters (TABLE. 3.1) have been explored.

Table 3.1: Summary of model parameters. The 'units' depends on the scale of particular agents, for instance, r_r may be small for an insect but much larger for a wild goose.

Parameter	Unit	Symbol	Value
Number of individuals	None	N	100
Repulsion Radius	Units	r_r	1
Orientation Radius	Units	δr_o	0-15
Attraction Radius	Units	δr_a	0-15
Blind volume	Degrees	β	90
Maximum turning rate	Degrees/second	θ	40
Time step increment	Seconds	τ	0.1-0.5
Maximum speed	Units/second	v_0	8-50

Table 3.2: Illustration of important performance indices. M denotes the number of experiments, M' denotes the number of convergent experiments, N is the number of agents.

Parameter	Symbol	Expression	Definition
Group polarization	$p(t)$	$p(t) = \frac{1}{N}\left\|\sum_{i=1}^{N}\vec{d}_i(t)\right\|$; $0 \le p(t) \le 1$	Average direction of all the agents at time t, approaches 1 as converging; on the contrary, $p(t)$ approaches 0. p measures the convergence the group has achieved.
Convergence ratio	CR	$CR = \frac{M'}{M}$	The ratio that a group of randomly initialized agents will finally reach global convergence;

3.4.1 Performance Indices

Convergence ratio (CR) and group polarization (p), are extensively investigated throughout the paper to evaluate convergence performance. As shown in Table. II, the larger value of CR or p represents the better convergence performance.

3.4.2 Performance Analysis

Figure 3.6 demonstrates how adaptive degree ϕ evolves with time t in the improved adaptive-velocity model in Eq.(3.10). ϕ decreases when the system undergoes from random to alignment corresponding to the convergent process shown in Figure. 3.5. Figure. 3.7 demonstrates that the system with adaptive and weighted strategies converges faster when applied to the Couzin model. In the constant-ϕ model [11], as shown in Figure. 3.7, 3.8, when ϕ is chosen small, the high-speed performance is not improved observably; while when ϕ increases, the convergence is prominently decelerated. However, the curve corresponding to the improved adaptive-velocity model ($\phi = tan(\delta/2)$) is above the curves of constant-ϕ models in Figure. 4. Furthermore, as shown in Figure. 5(b), at high speeds, for example, at $v_0 = 18$, although the Couzin model ($\phi = 0$) can hardly achieve global convergence as $CR \approx 0$, the convergence ratio CR is still at a large value for the improved adaptive-velocity model ($\phi = tan(\delta/2)$), even without any leader or other global information. These results reveal the ability of the improved adaptive-velocity model to maintain fast convergence and improve the high-speed performance simultaneously.

As shown in Figure 3.9, when the weighted strategy is applied (the model is called the weighted adaptive model), the system which has not achieved convergence is in a relatively small region with strong connectivity of the communication network. As shown in Figure. 3.10, p and CR of the weighted adaptive model remain large at $v_0 = 22$, where p and CR in other models are very small. To investigate the system performance in super high-speed conditions ('super high speed' is defined as $v \geq 22$), the upper bound of v_0 is extended to 1500. As shown in Figure 3.11, the weighted adaptive model keeps $p \geq 0.8$ even at $v_0 \approx 200$. Furthermore, the improvement of the high-speed performance is not at the cost of convergent time. The curve

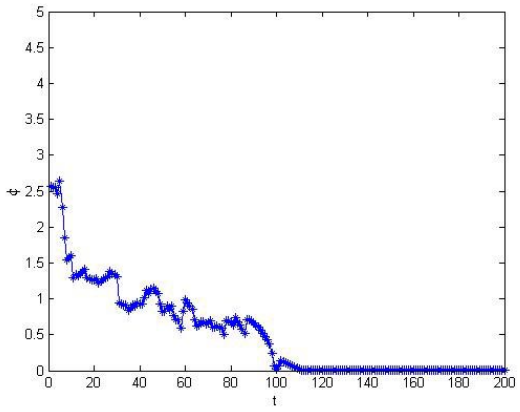

Figure 3.6: The process that the adaptive degree $\phi(t)$ evolves with t in one experiment, $v_0 = 20$.

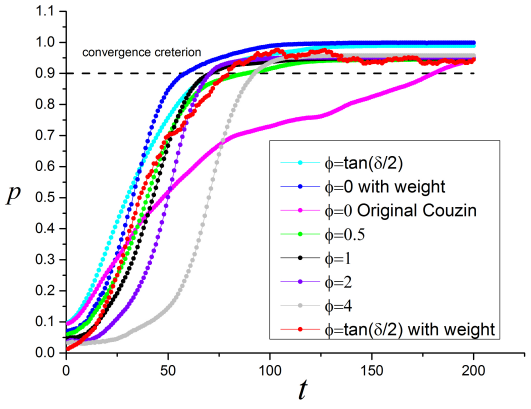

Figure 3.7: The evolving process of the group polarization p from initial random state to convergence in different models, $v_0 = 20$. the system state is said convergence when $p \geq 0.9$.

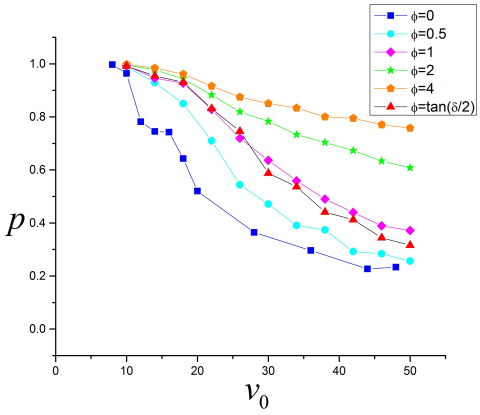

(a) Group polarization p versus the set speed

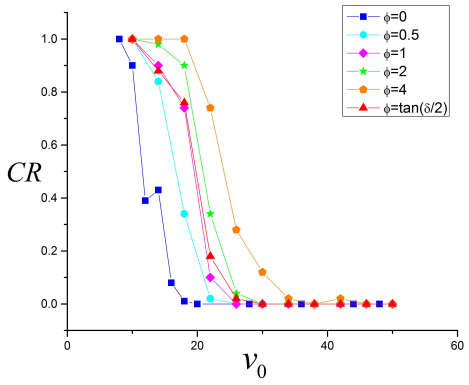

(b) Convergence ratio CR versus the set speed

Figure 3.8: Group polarization p and convergence ratio CR in the Couzin model ($\phi = 0$). the constant-ϕ model when ϕ is assigned 0.5, 1, 2, 4 and the improved adaptive-velocity Couzin model $\phi = tan(\delta/2)$. $\Delta r_o = 14$, $\Delta r_a = 14$. Experiments are averaged over 50 trials.

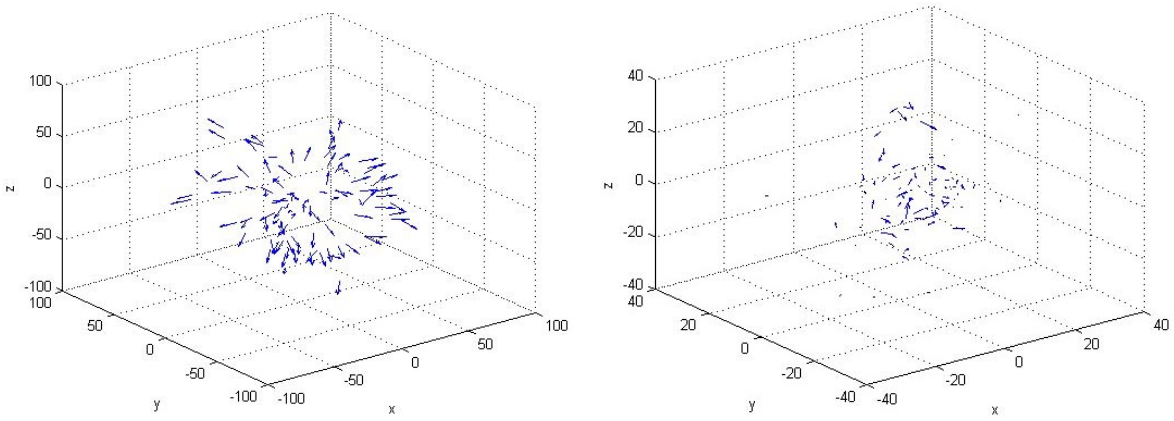

(a) The Couzin model

(b) With the improved adaptive-velocity and the weighted strategies

Figure 3.9: Divergent behaviors at the 10^{th} step, $v_0 = 160$.

($\phi = tan(\delta/2)$ with weight) in Figure. 4 demonstrates that the weighted adaptive model also has fast convergence.

3.4.3 Further Exploration of the Weighted Adaptive Model

As a function of agents' speeds, define E_k as the system kinetic energy in flocking systems:

$$E_k(t) = \sum_{i=1}^{N} \frac{1}{2} m v_i(t)^2 \tag{3.12}$$

Assuming the mass of agents is uniform, $m = 1$, $E_k(t)$ of the original Couzin model remains a constant because the agents' speed is a constant number as in Figure 3.12. With a larger adaptive degree ϕ, E_k is smaller in initial random state. The weighted adaptive model exhibits a very low energy cost at the initial state. During the converging process, the kinetic energy/speed increases gradually compared to the steep rise in the constant-ϕ model [11] when $\phi = 4$. The gradual increase is friendly to devices in artificial flocking systems.

System convergence performance varies with Δr_o and Δr_a in the Couzin model [9].

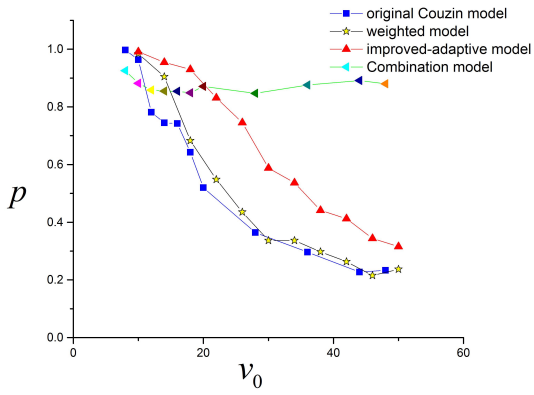

(a) Group polarization p versus the set speed

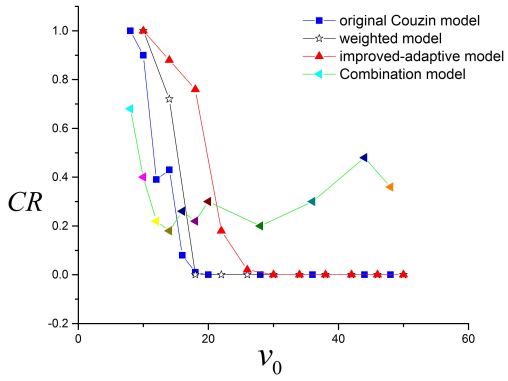

(b) Convergence ratio CR versus the set speed

Figure 3.10: p and CR in the Couzin model, the improved adaptive-velocity model, the weighted model and the combination model (the weighted adaptive Couzin model). Experiments are averaged over 50 trails.

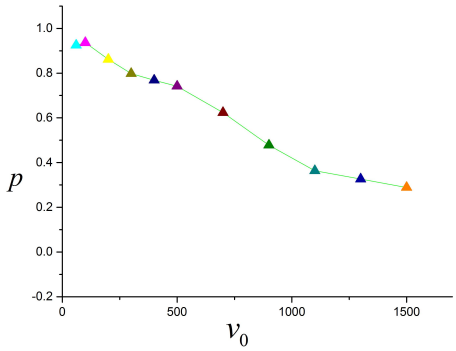

(a) Group polarization p versus the set speed

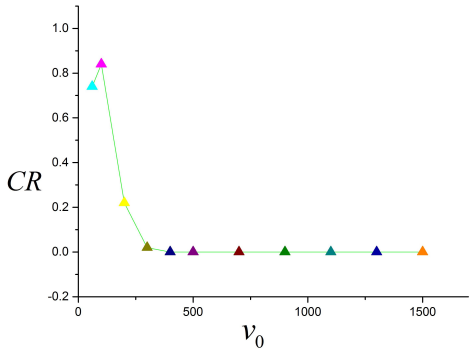

(b) Convergence ratio CR versus the set speed

Figure 3.11: Further exploration of p and CR in very high speed conditions in the weighted adaptive Couzin model, v_0 ranges from 0 to 1500. Experiments are averaged over 50 trials.

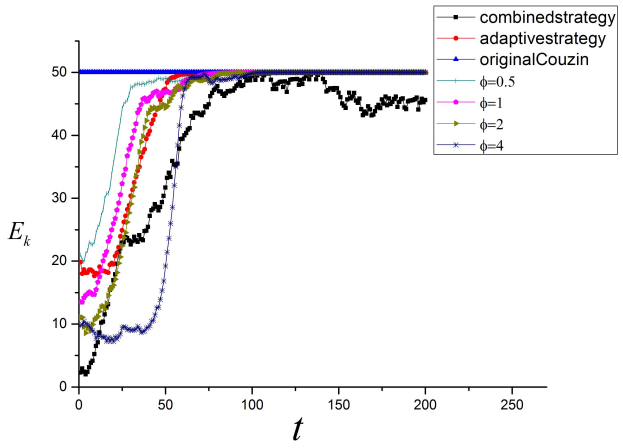

Figure 3.12: The kinetic energy E_k as a function of time t for different adaptive degrees ϕ, $v_0 = 10$, for every agent, $m = 1$. Experiments are averaged over 50 trails.

p as a crucial performance index increases when both Δr_o and Δr_a increase shown in Figure 3.13. In the weighted adaptive model, the tendency is similar but more gradual than in the original Couzin model.

The system performance is also influenced by the time step increment τ in the simulation. Figure 3.14 shows that the convergence performance gets worse (p and CR decrease) as τ increases, i.e., the system will hardly converge when the value of τ is large.

3.5 Conclusion

This chapter presents some classical collective behavior models and their properties. To avoid their defects, and in the meantime, inherit their advantages, we proposed an improved adaptive-velocity strategy and applied it to the Couzin model. Then, we investigated its high-speed system performance. In addition, the communication network is rendered heterogeneous by assigning weights to further improve

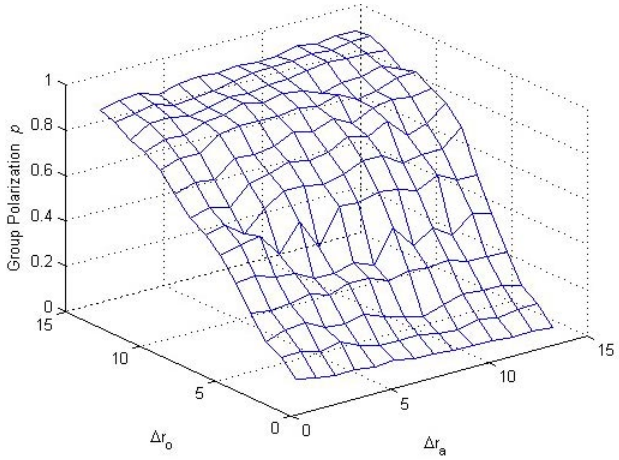

Figure 3.13: Group polarization p changes with Δr_o and Δr_a, other parameters are the same as Figure. 3(E) in [9]. Experiments are averaged over 50 trials.

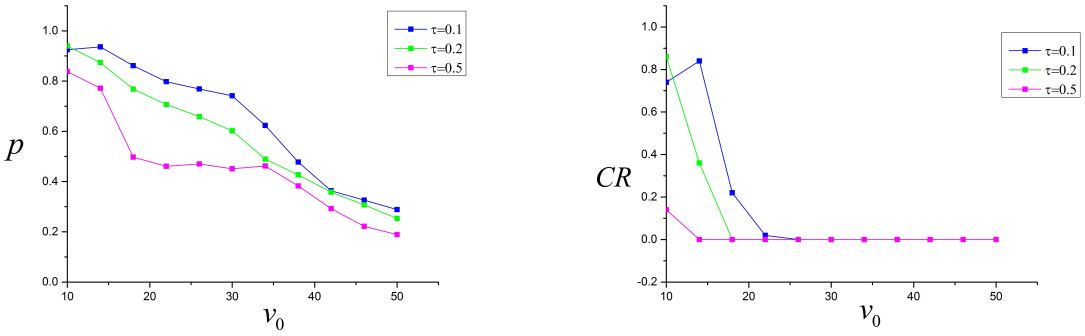

(a) Group polarization p versus the set speed

(b) Convergence ratio CR versus the set speed

Figure 3.14: p and CR correspond to different iteration time interval τ. Experiments are averaged over 50 trials.

its performance. Simulation results illustrate that the improved adaptive-velocity model has enhanced high-speed system performance and achieved quick convergence simultaneously. After adopting the weighted strategy, the weighted adaptive model exhibits the ability to quickly converge at super-high speeds with low energy consumption. Further exploration has been made to investigate the parameter space of the weighted adaptive model. The weighted adaptive model has jitters after the system has converged as shown in Figure 3.7 and Figure 3.10. Some important issues about the models in this paper remain to be considered. For example, the influence of the improved adaptive-velocity strategy and the weighted strategy to the torus convergence [9].

The improved adaptive-velocity and the weighted strategies reflect animal intelligence, which is deemed ultimately important in modeling flocking behaviors. This chapter proposes two promising strategies for flocking models with simple distributed decision-making rules and provides ideas for bio-inspired engineering and artificial intelligent control for multi-agent systems.

4. SEMI-GLOBAL OUTPUT REGULATION FOR HETEROGENEOUS NETWORKS WITH INPUT SATURATION VIA LOW GAIN FEEDBACK

In this section, we discuss the output regulation of linear multi-agent systems with consideration of input saturation. The overall system consists of multiple agents. The virtual leader is the exosystem, while the others are from the multi-agent plant. The agents communicate with each other following the topology of the network. By devising a distributed observer, we can solve the problem with state feedback. This problem can also be viewed as a generalization of some results of the leader-following consensus problem of multi-agent systems.

4.1 Problem Statement

4.1.1 Model

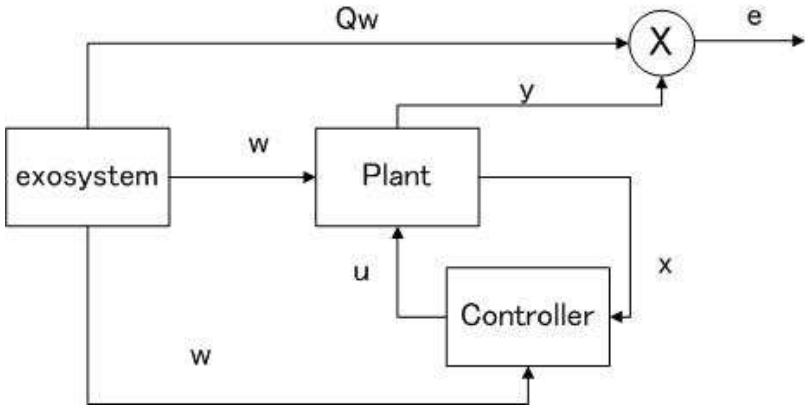

Figure 4.1: Output regulation problem flow chart

Consider a group of N agents with general linear dynamics with input saturation, labeled as $1, 2, \ldots, N$. As shown in Figure 4.1, an external system which is called

the exosystem is connected to this multi-agent plant. The motion of each agent is described in the following:

$$\begin{aligned} \dot{x}_i &= A_i x_i + B_i \sigma(u_i) + D_i w, \\ \dot{w} &= sw, \\ e_i &= C_i x_i + M_i \sigma(u_i) + Q_i w \end{aligned} \qquad i = 1, 2, \ldots, N, \tag{4.1}$$

where $x_i \in \mathrm{R}^n$ is the state of agent i, $w \in \mathrm{R}^q$ is the state of the exosystem, $e_i \in \mathrm{R}^p$ is the tracking error between the output $(C_i x_i + M_i u_i)$ and the reference signal $-Q_i w$, $u_i \in \mathrm{R}^m$ is the control input acting on agent i. $A_i \in \mathrm{R}^{n\times n}$, $B_i \in \mathrm{R}^{n\times m}$, $D_i \in \mathrm{R}^{n\times q}$, $C_i \in \mathrm{R}^{p\times n}$, $M_i \in \mathrm{R}^{p\times m}$, $Q_i \in \mathrm{R}^{p\times q}$. $D_i w$ denote the disturbance of the i_{th} subsystem from the exosystem, and $\delta : \mathrm{R}^m \to \mathrm{R}^m$ is a saturation function [26] defined as

$$\begin{aligned} &\delta(u_i) = [\mathrm{sat}(u_{i1}) \;\; \mathrm{sat}(u_{i2}) \;\; \ldots \;\; \mathrm{sat}(u_{im})]^{\mathrm{T}}, \\ &\mathrm{sat}(u_{ij}) = \mathrm{sgn}(u_{ij}) \min\{|u_{ij}|, \Delta\} \end{aligned} \tag{4.2}$$

for some constant $\Delta > 0$.

Not all the agents in the multi-agent network have access to the information of the exosystem directly. The exosystem can be treated as a virtual leader. We construct a distributed observer to estimate the exosystem state w

$$\begin{aligned} \dot{\hat{w}}_i &= s\hat{w}_i + \mu[\sum_{j\in N_i} a_{ij}(\hat{w}_j - \hat{w}_i) + h_i(w - \hat{w}_i)], \\ \dot{x}_i &= A_i x_i + B_i \delta(u_i) + D_i \hat{w}_i, \end{aligned} \tag{4.3}$$

where $\hat{w}_i \in \mathrm{R}^q$ is the state of the observer of agent i and μ is some positive number. Define the adjacency matrix $\Lambda_{\theta(t)} = \{a_{ij\theta(t)}\}$ of graph G as $a_{ij\theta(t)} = 1$ if $(j, i) \in E_{\theta(t)}$, and $a_{ij\theta(t)} = 0$ otherwise. The connectivity between the virtual leader and agents are represented by a matrix $H_{\theta(t)} = diag\{h_1(t), h_2(t), \ldots, h_N(t)\}$, where $\theta : [0, \inf) \to \Theta$

is a switching signal whose value at time t is the index of the graph at time t and Θ is finite. If agent i can receive the information of the exosystem, it is treated as a neighbor of the virtual leader and $h_i(t) = 1$; otherwise, $h_i(t) = 0$.

The following notation is used throughout this paper. I_n is the identity matrix of order n and $\otimes$ stands for the Kronecker product. The superscript T means transpose for real matrices. The notation $Q > 0$ denotes a positive definite matrix Q, and the notation $Q \geq 0$ denotes a nonnegative definite matrix Q.

4.1.2 Related Graph Theories in Switching Network

The switching network consisting of N agents is described by an undirected graph $G = \{V, E_{\theta(t)}\}$ [41]. In this graph, the set of vertices $V = \{1, 2, \ldots, N\}$ represents the agents in the group and the edge denoted by the pair (i, j) represents a dynamic communication link between i and j. A graph is said to contain a spanning tree with a root if every vertex of the graph can be reached from the root vertex. The Laplacian matrix of graph G with adjacency matrix $\Lambda_{\theta(t)}$ is given by $L_{\theta(t)} = \Phi(\Lambda_{\theta(t)}) - \Lambda_{\theta(t)}$, where the degree matrix $\Phi(\Lambda_{\theta(t)})$ is a diagonal matrix with ith diagonal elements $\sum_{j=1, j\neq i}^{N} a_{ij\theta(t)}$.

Lemma 1 *[20] Let L be the symmetric Laplacian of an undirected graph G consisting of N agents. Let $\bar{G}$ be the graph consisting of the N agents and the virtual leader and containing a spanning tree with the leader as the root vertex. Then $L + H > 0$, where $H = diag\{h_1, h_2, \ldots, h_N\}$.*

Lemma 2 *[41] Let L_1 and L_2 be the symmetric Laplacians of graph G_1 and G_2 consisting of N agents, respectively. Let $\bar{G}_1$ be a graph consisting of the N agents and a leader and containing a spanning tree. Let $\bar{G}_2$ be a graph generated by adding some edge(s) among the N agents into $\bar{G}_1$. Then, $\lambda_1(L_2 + H) \geq \lambda_1(L_1 + H) > 0$, λ_1 denotes the minimal eigenvalue.*

Remark 1 *Let $\bar{G}_s$ be the spanning tree consisting of N agents and a leader, L_s the Laplacian of the communication graph consisting of the N agents. $\{\bar{G}_i\}$ denotes a set of graphs generated by adding some edge(s) among the N agents to $\bar{G}_s$. Then $\lambda_1(L_s + H) \leq \lambda_1(L_i + H) > 0$*

Lemma 3 *Let $\bar{G}$ be a spanning tree consisting of N agents and a leader and L_s is the Laplacian of the communication graph consisting of the N agents, $\bar{G}_m$ be the minimal spanning tree with leader being its root and L_m is its Laplacian. Suppose S is a given matrix. There exists a $\mu^* > 0$, such that $\mu^* \lambda_i(L_m + H_m) > \lambda_j(S)$, for all $i, j = 1, 2, \ldots, N$, L_m and H_m are the corresponding matrices for the minimal spanning tree. Then, for all $\mu \geq \mu^*$, $\lambda_i(S) - \mu\lambda_j(L + H) < 0$.*

proof. By Lemma 2, $0 < \lambda_1(L_m + H_m) \leq \lambda_1(L + H)$, where λ_1 represents the minimal eigenvalue. If $\mu^* \lambda_1(L_m + H_m) > \lambda_j(S)$, then $\mu^* \lambda_1(L + H) > \lambda_j(S)$. Furthermore, for all $\mu \geq \mu^*$, $\mu\lambda_i(L + H) > \lambda_j(S)$ for all $i = 1, 2, \ldots, N$. □

Lemma 4 *Let L be the symmetric Laplacian of an undirected graph G consisting of N agents. Let $\bar{G}$ be the graph consisting of the N agents and the virtual leader and containing a spanning tree with the leader as the root vertex. Then $(L + H) \otimes 1_N = H \otimes 1_N$, where $H = diag\{h_1, h_2, \ldots, h_N\}$ and 1_N is an $N \times 1$ column vector whose elements are all 1.*

proof. For any L as the Laplacian matrix of an undirected graph, the i_{th} element in $L \otimes 1_N$ is $\sum_{j=1}^{N} a_{ij} = 0$. □

4.1.3 Objective

The problem of output regulation with input saturation for the multi-agent system described above is given in Definition 1.

Definition 1 *(Semi-global Linear Cooperative Output Regulation Problem): For any* a priori *given bounded set $\mathcal{X} \subset \mathrm{R}^n$ and $W \subset R^q$, find a control law u_i for each agent*

i in system Eq. (4.1), which uses only local information from neighbor agents, such that

(1)the overall closed-loop system is exponentially stable;

(2)For any initial condition $x_i(0) \in \mathcal{X}$ for all $i = 1, 2, \ldots, N$ and $w \in W$, the tracking error $\lim_{t\to\infty} e_i(t) = 0$, $i = 1, 2, \ldots, N$.

4.2 Solvability Assumptions

Assumption 1 *(ANCBC) The pair (A_i, B_i) are stabilizable, and all the eigenvalues of A_i are in the closed left half s-plane, $i = 1, 2, \ldots, N$.*

Assumption 2 *There exist matrices Π_i and Γ_i, such that*

$$\begin{cases} \Pi_i s = A_i\Pi_i + B_i\Gamma_i + D_i \\ C_i\Pi_i + M_i\Gamma_i + Q_i = 0 \end{cases}, i = 1, 2, \ldots, N. \tag{4.4}$$

Assumption 3 *There exists a $\sigma > 0$ and $T \geq 0$, such that $\|\Gamma\hat{w}_i\|_{\infty,T} \leq \Delta - \sigma$, for all $i = 1, 2, \ldots, N$.*

Lemma 5 *[26] Let Assumption 1 hold, then there exists unique $P_i(\varepsilon) > 0$, which are the solutions to the algebraic Riccati equation (ARE)*

$$\begin{aligned} &A_i^T P_i(\varepsilon) + P_i(\varepsilon)A_i - P_i(\varepsilon)B_iB_i^T P_i(\varepsilon) + \varepsilon I = 0, \\ &i = 1, 2, \ldots, N \end{aligned} \tag{4.5}$$

with $\lim_{\varepsilon\to 0} P_i(\varepsilon) = 0$.

Assumption 4 *There exists a spanning tree in the graph $\bar{G}$ consisting of N agents and a leader with the leader being the root.*

Assumption 5 *s has no eigenvalues with negative real parts.*

4.3 Control Law Designed via Low Gain State Feedback

4.3.1 Low Gain Feedback Technique

Low gain feedback was introduced by Lin etc. [26]. In the classical control theory of single input single output systems, it is known that well-designed high gain feedback systems have the advantages of high steady-state accuracy consistent with stability, fast response, disturbance rejection, and insensitivity to parameter uncertainties and distortions. The concept underlying high gain feedback is that of asymptotics and, hence, by high gain feedback we mean a family of feedback laws in which a parameterized gain matrix, say $F(e)$, approaches infinity as the parameter approaches its extreme value (typically zero or infinity). Consequently, the implementation of high gain feedback laws entails large control inputs (either in magnitude or in energy) and hence large actuation capacities.

Low gain feedback has been conceived to either avoid or to complement high gain feedback whenever such "unpleasant" features of high gain feedback prevent certain control objectives from being achieved. In the past few years, several low gain design methods have been developed by Lin etc. [26] to achieve various control objectives that high gain feedback (or high gain feedback alone) could not achieve. These objectives include control of linear systems subject to actuator magnitude and/or rate saturation and semi-global stabilization of minimum phase input-output linearizable nonlinear systems.

Similar to that of high gain feedback, the concept underlying low gain feedback is also that of asymptotics and, roughly speaking, by low gain feedback we mean a family of feedback laws in which a parameterized gain matrix, say $F(\varepsilon)$, approaches zero as the parameter ε approaches zero. In the development of low gain feedback design techniques, one observes that the closed-loop system properties induced by the

low gain feedback are often mirror images of those induced by the high gain feedback, and are beautifully symmetric to each other. For example, high gain feedback induces fast time scales while low gain feedback induces slow ones.

It is known that a linear time-invariant system subject to actuator saturation can be globally asymptotically stabilized if and only if it is asymptotically null controllable with bounded controls (ANCBC).

Consider a linear system subject to actuator magnitude saturation described by:

$$\begin{cases} \dot{x} = Ax + B\delta(u) \\ \qquad y = Cx \end{cases} \tag{4.6}$$

where $x \in R^n$ is the state, $u \in Rm$ is the control input to the actuators, $y \in R^p$ is the measurement output, and $\delta : R^m \to R^m$ is a saturation function, as defined in the 4.2. 1 holds.

Assumption 6 *: The pair (A, C) is detectable.*

The problems that we are to solve using low gain feedback are the following: Consider system in Eq. (4.6) with δ is a saturation function. For any a priori given bounded set of initial conditions $\mathcal{X} \subset R^n$, find a state feedback law $u = F_{\mathcal{X}}x$ such that, for any δ within the saturation bound, the equilibrium $x = 0$ of the closed-loop system is locally exponentially stable with $\mathcal{X}$ contained in its basin of attraction.

Algebraic Racatti Equation (ARE) Based Design:

Step 1 - State Feedback Design For the matrix pair (A, B), construct a family of low gain state feedback laws as,

$$u = -B'P(\varepsilon)x \tag{4.7}$$

where $P(\varepsilon) > 0$ is the solution to the H_2-ARE

$$A'P + PA - PBB'P + \varepsilon I = 0, \varepsilon \in (0, 1] \tag{4.8}$$

The existence of such a $P(\varepsilon)$ is guaranteed by Assumption 3.3.1.

Theorem 2. Consider system in Eq. (4.6) with δ a saturation function. If Assumption 3.3.1 is satisfied, then the family of state feedback laws in Eq. (4.7) solves Problem 3.3.1.

4.3.2 Control Law Design

Construct a state feedback law for agent i, define $F_i(\varepsilon) = -B_i^T P_i(\varepsilon)$

$$\begin{aligned} &u_i = F_i(\varepsilon)x_i + (-F_i(\varepsilon)\Pi_i + \Gamma_i)\hat{w}_i, \\ &i = 1, 2, \ldots, N \end{aligned} \tag{4.9}$$

$P_i(\varepsilon)$ is the solution to the ARE (4.8) in Lemma 5.

Theorem 1 *Consider a multi-agent system with N agents and a leader with dynamics givenly (4.1). Then under Assumptions 1, 2, 3, 4 and 5, the semi-global cooperative output regulation of switching networks can be solved by the distributed dynamic state feedback control law (4.9) with sufficiently large positive number ε.*

Proof. Define $\xi_i = x_i - \Pi_i \hat{w}_i$, then rewrite u_i as a function of ξ_i

$$\begin{aligned} u_i(\xi_i) &= F_i(\varepsilon)\xi_i + F_i(\varepsilon)\Pi_i\hat{w}_i + (-F_i(\varepsilon)\Pi_i + \Gamma_i)\hat{w}_i \\ &= F_i(\varepsilon)\xi_i + \Gamma_i\hat{w}_i \end{aligned} \tag{4.10}$$

From Assumption 3, $\|\Gamma\hat{w}_i\|_{\infty,T} \geq \Delta - \sigma$, for all $i = 1, 2, \ldots, N$. Moreover, $\xi_i(0)$ is bounded by initialization and $\xi_i(T)$ is determined by a linear differential

equation with bounded input $\delta(u_i)$ and $\Gamma_i\hat{w}_i$, thus $\xi_i(t)$ is bounded for $t \in (0, T]$, $\xi_i(t) \in \Xi_i$ denotes its bound. Then pick a positive definite Lyapunov function $V(\xi) = \sum_{i=1}^{N} \xi_i^T P_i(\varepsilon)\xi_i$ where $\xi = [{\xi_1}^T, \ldots, {\xi_N}^T]^T$, and let $c > 0$ be such that

$$c \geq \sup_{\xi_i \in \Xi_i, \varepsilon \in (0,\Delta], i=1,\cdots,N} V(\xi) \tag{4.11}$$

Such a c exists since $\lim_{\varepsilon \to 0} \bar{P}_i(\varepsilon) = 0$ and Ξ_i are bounded and independent of ε, therefore, there exists an ε_1^* such that $\eta_i \in L_V(c)$ implies that for any $\varepsilon \in [0, \varepsilon_1^*]$, $\|F_i(\varepsilon)\xi_i\|_\infty \leq \sigma$. Thus, $\|u_i(\xi_i)\| = \|F_i(\varepsilon)\xi_i + \Gamma_i\hat{w}_i\| < \Delta - \sigma + \sigma = \Delta$. Then, $\delta(u_i) = u_i$ when $\xi_i(t) \in \Xi_i$.

Hence, for $t \geq T$ and $\xi_i \in L_V(c)$, the dynamics of ξ_i is given by

$$\begin{aligned}
\dot{\xi}_i &= A_i(\xi_i + \Pi_i\hat{w}_i) + B_i u_i(\xi_i) + D_i w - \Pi_i s\hat{w}_i \\
&\quad -\mu\Pi_i[\sum_{j\in N_i} a_{ij}(\hat{w}_j - \hat{w}_i) + h_i(w - \hat{w}_i)] \\
&= A_i(\xi_i + \Pi_i\hat{w}_i) + B_i F_i(\varepsilon)\xi_i + B_i\Gamma_i\hat{w}_i + D_i\hat{w}_i - D_i\hat{w}_{ei} \\
&\quad -\Pi_i s\hat{w}_i - \mu\Pi_i[\sum_{j\in N_i} a_{ij}(\hat{w}_j - \hat{w}_i) + h_i(w - \hat{w}_i)] \\
&= (A_i + B_i F_i(\varepsilon))\xi_i + (A_i\Pi_i + B_i\Gamma_i + D_i - \Pi_i s)\hat{w}_i \\
&\quad -D_i\hat{w}_{ei} - \mu\Pi_i[\sum_{j\in N_i} a_{ij}(\hat{w}_j - \hat{w}_i) + h_i(w - \hat{w}_i)] \\
&= (A_i + B_i F_i(\varepsilon))\xi_i - D_i\hat{w}_i + D_i w \\
&\quad -\mu\Pi_i[\sum_{j\in N_i} a_{ij}(\hat{w}_j - \hat{w}_i) + h_i(w - \hat{w}_i)], \\
&\quad i = 1, 2, \ldots, N
\end{aligned} \tag{4.12}$$

Let $A = block[diag(A_1, \ldots, A_N)]$, $B = block[diag(B_1, \ldots, B_N)]$, $\Pi = block[diag(\Pi_1, \ldots, \Pi_N)]$, $P_\alpha(\varepsilon) = block[diag(P_1(\varepsilon), \ldots, P_N(\varepsilon))]$, $F(\varepsilon) = block[diag(F_1(\varepsilon), \ldots, F_N(\varepsilon))]$, $S = s \otimes I_p$, $\eta = [{\eta_1}^T, \ldots, {\eta_N}^T]^T$, $\bar{w} = 1_N \otimes w$. Because $\sum_{i=1}^{N} \sum_{j\in N_i} a_{ij}(\hat{w}_j - \hat{w}_i) = -(L \otimes I_q)\hat{w}$, $H = \text{block } diag(h_1, \ldots, h_N)$. Because $H \otimes 1_N = (L + H) \otimes 1_N$, where 1_N is defined as an $N \times 1$ column vector whose elements are all 1. Rewrite the dynamics of the

closed-loop system in compact form

$$\begin{aligned}\dot{\xi} &= [A+BF(\varepsilon)]\xi + [\mu\Pi(L\otimes I_q) - D]\hat{w} \\ &\quad -[\mu\Pi(L\otimes I_q) - D]\bar{w} \\ \dot{\hat{w}} &= (I_N \otimes S)\hat{w} - \mu(L\otimes I_q)\hat{w} + \mu(L\otimes I_q)\bar{w}\end{aligned} \tag{4.13}$$

$$\begin{aligned}\begin{bmatrix} \dot{\xi} \\ \dot{\hat{w}} \end{bmatrix} &= \underbrace{\begin{bmatrix} A+BF(\varepsilon) & \mu\Pi(L\otimes I_q) - D \\ 0 & I_N \otimes S - \mu(L\otimes I_q) \end{bmatrix}}_{A_{cl}} \begin{bmatrix} \xi \\ \hat{w} \end{bmatrix} \\ &\quad + \underbrace{\begin{bmatrix} D - \mu\Pi(L\otimes I_q) \\ \mu(L\otimes I_q) \end{bmatrix}}_{B_{cl}} \bar{w}\end{aligned} \tag{4.14}$$

Define a Lyapunov function

$$V_{cl} = \begin{bmatrix} \xi^T & \hat{w}^T \end{bmatrix} \begin{bmatrix} P_\alpha & 0 \\ 0 & P_\beta \end{bmatrix} \begin{bmatrix} \xi \\ \hat{w} \end{bmatrix} \tag{4.15}$$

Where P_α is defined as the collective form of $P_i(\varepsilon)$, P_β is a positive definite matrix. Then, the derivative of V_{cl} is as follows:

$$\begin{aligned}\dot{V}_{cl} &= \begin{bmatrix} \xi^T \\ \hat{w}^T \end{bmatrix}^T (A_{cl}^T \begin{bmatrix} P_\alpha & 0 \\ 0 & P_\beta \end{bmatrix} \\ &\quad + \begin{bmatrix} P_\alpha & 0 \\ 0 & P_\beta \end{bmatrix} A_{cl}) \begin{bmatrix} \xi \\ \hat{w} \end{bmatrix}\end{aligned} \tag{4.16}$$

$$
\begin{aligned}
Q &= A_{cl}^T \begin{bmatrix} P_\alpha & 0 \\ 0 & P_\beta \end{bmatrix} + \begin{bmatrix} P_\alpha & 0 \\ 0 & P_\beta \end{bmatrix} A_{cl} \\
&= \begin{bmatrix} Q_1 & Q_2 \\ Q_3 & Q_4 \end{bmatrix}
\end{aligned} \tag{4.17}
$$

$$
\begin{aligned}
Q_1 &= P_\alpha A + A^T P_\alpha - 2P_\alpha B B^T P_\alpha \\
Q_2 &= \mu \Pi (L \otimes I_q) - D \\
Q_3 &= \mu (L \otimes I_q)^T \Pi^T - D^T \\
Q_4 &= P_\beta [(I_N \otimes S) - \mu (L \otimes I_q)] \\
&\quad + [(I_N \otimes S)^T - \mu (L \otimes I_q)^T] P_\beta
\end{aligned}
$$

If the closed-loop system is asymptotically stable, Q should be negative definite. By choosing μ such that the eigenvalues of $(I_N \otimes S) - \mu(L \otimes I_q)$ are all negative, the following inequalities hold:

$$
\begin{aligned}
Q_1 &< 0 \\
Q_4 &< 0 \\
Q_2 Q_3 &= |\mu \Pi (L \otimes I_q) - D|^2 \\
det(Q_1 Q_4 - Q_2 Q_3) &> 0
\end{aligned} \tag{4.18}
$$

Therefore, by checking the leading principal minors of Q and $\lim_{\varepsilon \to 0} P_\alpha(\varepsilon) = 0$, there exists a $\varepsilon_2^* > 0$, such that Q is negative definite for any $\varepsilon \in (0, \varepsilon_2^*]$. For all $\varepsilon \in (0, min\{\varepsilon_1^*, \varepsilon_2^*\}]$ and $\mu > \mu^*$, when x and w are in priori given bounded sets $\mathcal{X} \subset \mathrm{R}^n$ and $W \subset \mathrm{R}^q$ respectively, A_{cl} is asymptotically such that ξ and $\hat{w}$ are both asymptotically stable. Then, $x = \xi + \hat{w}$ is semi-globally asymptotically stable. Thus,

objective 1 is satisfied.

Assume $[x^T \quad \hat{w}^T]^T = [\Pi\bar{w}^T \quad \bar{w}^T]^T$ is a solution to the closed-loop system. We have

$$\begin{aligned} \dot{x} &= Ax + Bu + C\bar{w} \\ &= (A + BF)x + (-BF\Pi + B\Gamma)\hat{w} + D\bar{w} \end{aligned} \tag{4.19}$$

The closed-loop dynamics is as follows.

$$\begin{aligned} \begin{bmatrix} \dot{x} \\ \dot{\hat{w}} \end{bmatrix} &= \begin{bmatrix} A + BF(\varepsilon) & -BF\Pi + B\Gamma \\ 0 & I_N \otimes S - \mu(L \otimes I_q) \end{bmatrix} \begin{bmatrix} \Pi\bar{w} \\ \bar{w} \end{bmatrix} \\ &+ \begin{bmatrix} D \\ \mu(L \otimes I_q) \end{bmatrix} \bar{w} \\ &= (I_N \otimes S) \begin{bmatrix} \Pi\bar{w} \\ \bar{w} \end{bmatrix} = (I_N \otimes S) \begin{bmatrix} x \\ \hat{w} \end{bmatrix} \end{aligned} \tag{4.20}$$

Define $A_c \triangleq \begin{bmatrix} A + BF(\varepsilon) & -BF\Pi + B\Gamma \\ 0 & I_N \otimes S - \mu(L \otimes I_q) \end{bmatrix}$. From Assumption 5, the eigenvalues of A_c and $I_N \otimes s$ do not coincide, thus $[x^T \quad \hat{w}^T]^T$ is the unique solution. Thus the closed-loop system has the same dynamics as the exosystem. From Eq. (4.1) and Assumption 2, the steady state tracking error

$$\begin{aligned} e &= Cx + Mu + Q\bar{w} \\ &= C\xi + C\Pi\hat{w} + MF(\varepsilon)\xi + M\Gamma\hat{w} + Q\bar{w} \\ &= (C\Pi + M\Gamma + Q)\bar{w} \\ &= 0 \end{aligned} \tag{4.21}$$

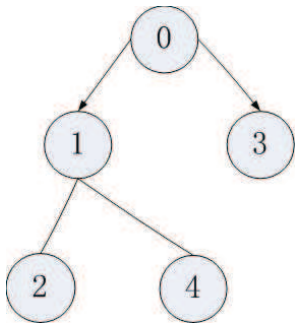

Figure 4.2: The interaction network.

Therefore, $e \to 0$ with $t \to +\infty$, and objective 2 is satisfied.

□

4.4 Numerical Examples

The simulation is performed with four agents and one leader that represents the exosystem. The multi-agent network is shown in Figure 4.2. The Laplacian L and H are as follows:

$$L = \begin{bmatrix} 2 & -1 & 0 & -1 \\ -1 & 1 & 0 & 0 \\ 0 & 0 & 0 & 0 \\ -1 & 0 & 0 & 1 \end{bmatrix}, H = \begin{bmatrix} 1 & 0 & 0 & 0 \\ 0 & 0 & 0 & 0 \\ 0 & 0 & 1 & 0 \\ 0 & 0 & 0 & 0 \end{bmatrix}$$

The exosystem is an unforced harmonic oscillator. The system matrices are

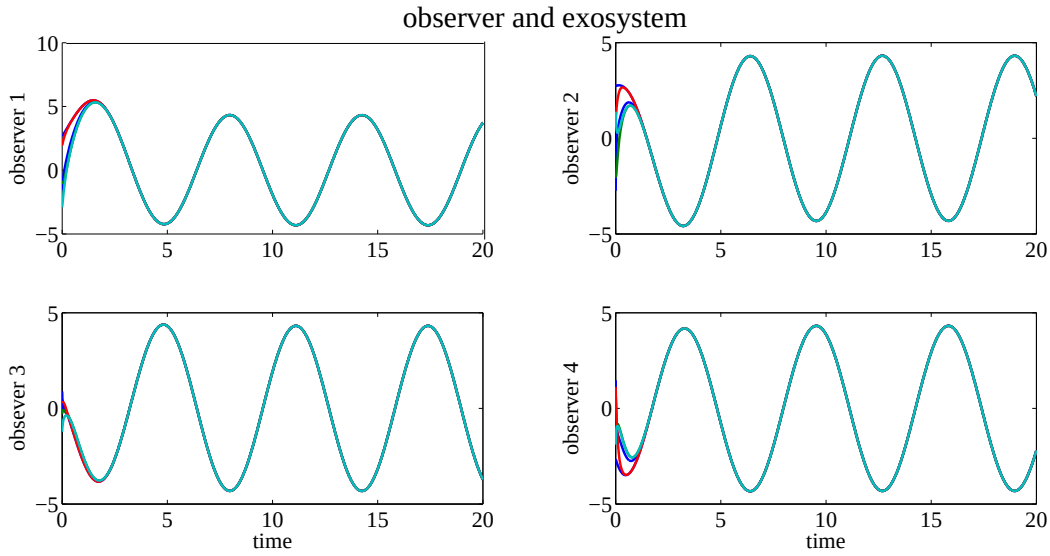

Figure 4.3: The observer and the exosystem

chosen as

$$A_i = \begin{bmatrix} -1 & 0 \\ 0 & 0 \end{bmatrix}, B_i = \begin{bmatrix} 0 \\ 1 \end{bmatrix}, D_i = \begin{bmatrix} 0 & 0 \\ 0 & 5 * i \end{bmatrix},$$
$$s = \begin{bmatrix} 0 & 1 \\ -1 & 0 \end{bmatrix}, C_i = [1 \quad 0], M_i = 5, Q_i = [-1 \quad 0]$$

(A_i, B_i) is asymptotically null controllable with bounded controls (ANCBC). The initial states x, w and $\hat{w}$ of every agent are randomly chosen from the box $[-3, 3] \times [-3, 3]$, $\Delta = 3$. We use the algorithm in [**?**] as a comparison, the control input is given by

$$u_i = K_{1i}x_i + K_{2i}\hat{w}_i, i = 1, \cdots, N \tag{4.22}$$

where K_{1i} is chosen to render let $A_i + B_iK_{1i}$ Hurwitz, and $K_{2i} = \Gamma_i - K_{1i}\Pi_i$. The plant state x, observer state $\hat{w}$ and the exosystem state w are shown in Figure 4.3.

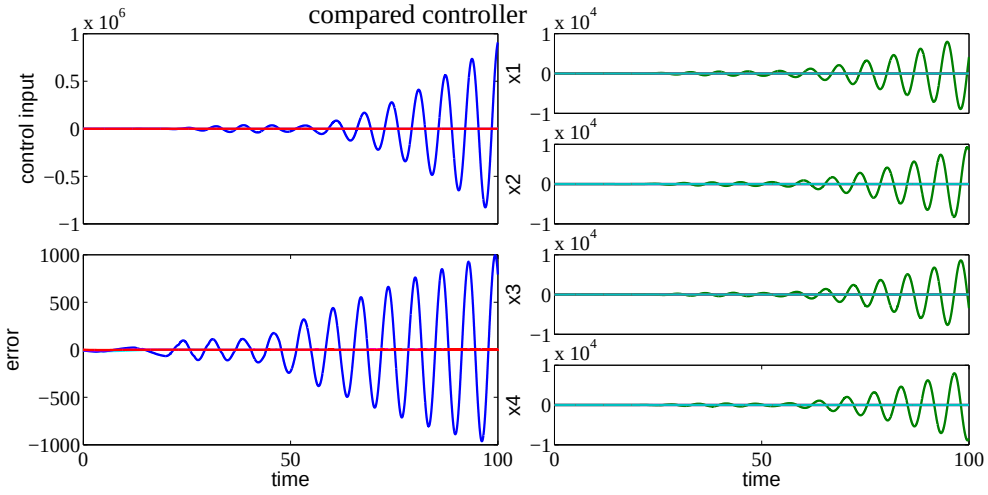

Figure 4.4: Error and control input with the compared controller

The error e and control input u for different values of ε are shown in Figure 4.4 and Figure 4.5.

4.5 Conclusion

In this chapter, we have studied the output regulation of linear multi-agent systems with input saturation. By devising distributed observers of the exosystem, we have solved the problem via a low gain feedback.

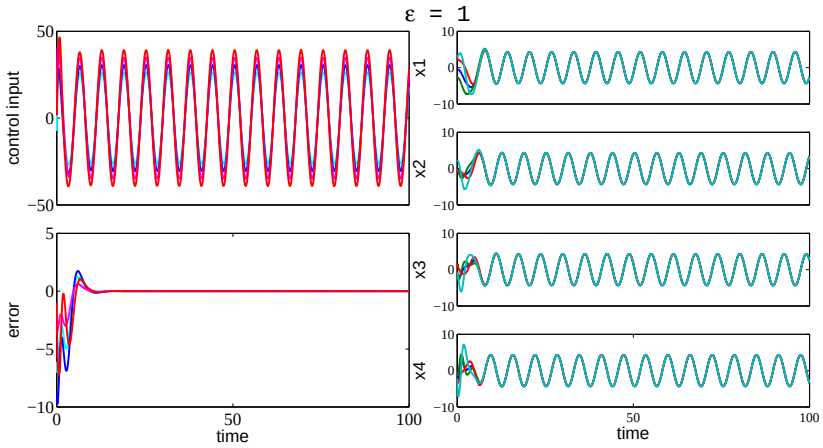

(a) error and control at ε = e-3

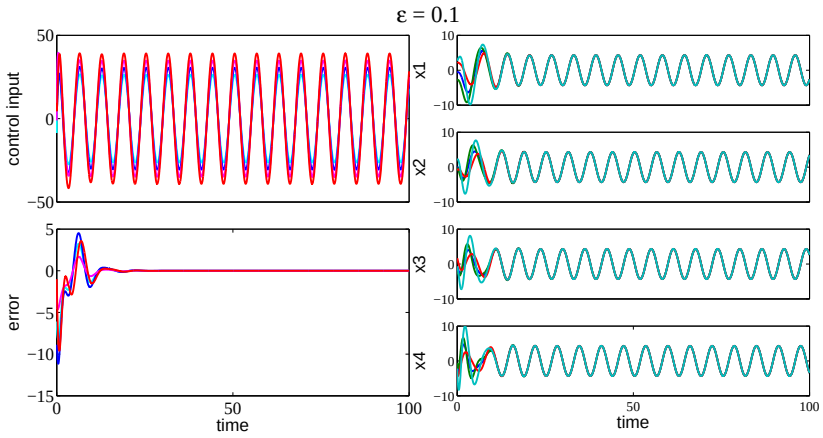

(b) error and control at ε = e-4

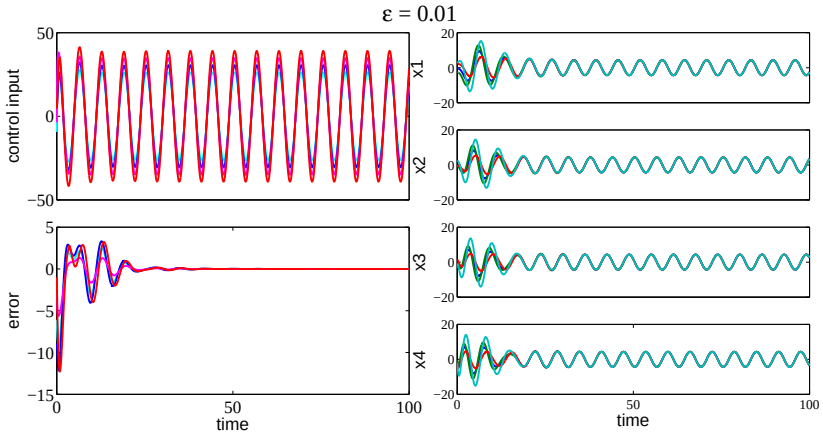

(c) error and control at ε = e-5

Figure 4.5: Error output and control input.

5. FLOCKING OF MULTIPLE-AGENTS WITH PRESERVED NETWORK CONNECTIVITY AND HETEROGENEOUS NONLINEAR DYNAMICS

Most previous works focus on linear systems especially systems with double-integrator dynamics [29, 32, 33, 42]. However, in reality, autonomous agents might be governed by more complicated nonlinear dynamics. In fact, in synchronization of complex dynamical networks, nonlinear dynamics is commonly used [13]. In [42], second-order consensus of agents with some homogeneous nonlinear dynamics was investigated in switching networks. This chapter has appeared as a research paper[1].

Many theoretical investigations in flocking of multiple agents tracking a (virtual) leader are formulated as a linear system or network with a fixed-coupling topology and uniform intrinsic agent dynamics. However, these conditions are difficult to satisfy or verify in a realistic flocking scenario. Therefore, a multi-agent system of flocking with heterogeneous nonlinear intrinsic dynamics is considered in this chapter, where network connectivity is preserved and the interconnection topology network based on the distance between agents varies with time. Furthermore, we extend the result to the multi-agent system with a nonlinear dynamical virtual leader. To keep all agents moving at the same velocity and guarantee stabilization of the distance between agents for collision avoidance, a connectivity-preserving algorithm combined with an artificial potential function for multiple agents are presented under the mild assumption that the initial network is connected. By using the proposed flocking algorithm, the multiple agents are made to move with the same velocity while preserving network connectivity, and in addition all agents' velocities can asymptotically

[1]Wang, M., Su, H., Zhao, M., Chen, M. Z., & Wang, H. (2013). Flocking of multiple autonomous agents with preserved network connectivity and heterogeneous nonlinear dynamics. Neurocomputing, 115, 169-177.

approach the velocity of the virtual leader effectively in a multi-agent system with a nonlinear dynamic virtual leader.

The remainder of the chapter is organized as follows. We first describe the model of the flocking system in Section 6.1. Our new results on the flocking problem are established in Section 6.2. Then some numerical simulation examples are presented to validate the effectiveness of the theoretical results in Section 6.3. Conclusions are drawn in Section 6.4.

5.1 Flocking Problems with Heterogeneous Nonlinear Dynamics

In our formulation, there are N agents, labeled $1, 2, 3, \ldots, N$. We denote $p_i \in \mathbf{R}^n$ as the position vector of agent i and $v_i \in \mathbf{R}^n$ as the velocity vector of agent i. These agents move in n-dimensional Euclidean spaces. The dynamic equations of each agent can be described as follows

$$\begin{aligned} \dot{p}_i &= v_i, \\ \dot{v}_i &= f_i(v_i) + u_i, \end{aligned} \tag{5.1}$$

where $f_i(v_i) \in \mathbf{R}^n$ is the intrinsic dynamic of agent $i, i = 1, 2, \ldots, N$ and $u_i \in \mathbf{R}^n$ is the control input of agent i. In particular, the intrinsic dynamics of multiple agents are heterogeneous and nonlinear.

5.2 Connectivity-Preserving Algorithm and Potential Function Design

To avoid fragmentation, we set up a connectivity-preserving flocking algorithm. Assuming that all agents have the same influencing/sensing radius $r > 0$, let $\varepsilon \in (0, r]$ be an arbitrarily small constant [42]. $G(t) = (\mathcal{V}, \mathcal{E}(t))$ is an undirected dynamic graph composed of a set of vertices $\mathcal{V} = 1, 2, \ldots, N$, denoting the set of agents and a time-varying set of edges $\mathcal{E}(t) = \{(i, j) | \, i, j \in V\}$.

Table 5.1: Algorithm 1: description of the indicator function.

Require	$\mathcal{E}(0) = \{(i,j) \mid \|p_i(0) - p_j(0)\| < r, i, j \in \mathcal{V}\}$ and $\sigma(i,j)[t^-] \in \{0,1\}$
1	**if** $\sigma(i,j)[t^-] = 1$ and $\|p_i(t) - p_j(t)\| \geq r$
2	**Then** $\sigma(i,j) = 0, i, j \in \mathcal{V}$
3	**else if** $\sigma(i,j)[t^-] = 0$ and $\|p_i(t) - p_j(t)\| \geq r - \varepsilon$
4	**Then** $\sigma(i,j) = 0, i, j \in \mathcal{V}$
5	**else if** $\sigma(i,j)[t^-] = 1$ and $\|p_i(t) - p_j(t)\| \leq r$
6	**Then** $\sigma(i,j) = 1, i, j \in \mathcal{V}$
7	**else if** $\sigma(i,j)[t^-] = 0$ and $\|p_i(t) - p_j(t)\| \leq r - \varepsilon$
8	**Then** $\sigma(i,j) = 1, i, j \in \mathcal{V}$
9	**end if**

5.3 Control Law Design

5.3.1 Flocking of Multiple Agents without a Virtual Leader

In this subsection, the flocking problem of multi-agent system without a virtual leader is investigated. In order to derive the main results, the following assumption is needed.

Assumption 7 *Suppose ℓ is a positive constant such that*

$$|f_i(v_i) - f_j(v_j)| \leq \ell, \quad \forall v_i, v_j \in \mathbf{R}^n i, j = 1, 2, \ldots, N. \tag{5.2}$$

Denote the central position and velocity of all the agents in the system in Eq. (5.1) by $\bar{p} = \frac{\sum_{i=1}^{N} p_i}{N}$ and $\bar{v} = \frac{\sum_{i=1}^{N} v_i}{N}$, respectively. Then the difference of position and velocity between agent i and the central of mass are given as $\hat{p_i} = p_i - \bar{p}$ and $\hat{v_i} = v_i - \bar{v_i}$, respectively. The control law is described by

$$
\begin{aligned}
u_i \quad &= -\sum_{j\in\mathcal{N}_i(t)} \nabla_{p_i}\psi\left(\|p_{ij}\|\right) \\
&\quad -\rho\sum_{j\in\mathcal{N}_i(t)} a_{ij}\left\{\operatorname{sgn}\left[\sum_{k\in\mathcal{N}_i(t)} a_{ik}(v_i-v_k)\right] -\operatorname{sgn}\left[\sum_{k\in\mathcal{N}_j(t)} a_{jk}(v_j-v_k)\right]\right\}
\end{aligned} \tag{5.3}
$$

where $\|p_{ij}\| = \|p_i - p_j\|$, ρ is the a positive constant, and $\mathcal{N}_i(t)$ denotes the neighborhood of agent i at time t, with explicit definition is

$$
\mathcal{N}_i(t) = \{j|\sigma(i,j)[t] = 1, j \neq i, j = 1, 2, \ldots, N\}. \tag{5.4}
$$

5.3.2 Potential Function

The nonnegative potential function $\psi\left(\|p_{ij}\|\right)$ is defined as a function of the distance $\|p_{ij}\|$ between agent i and agent j, differentiable with respect to $\|p_{ij}\| \in [0, r)$, satisfying

(1) $\psi\left(\|p_{ij}\|\right) \to \infty$ as $\|p_{ij}\| \to 0$ or $\|p_{ij}\| \to r$;

(2) $\psi\left(\|p_{ij}\|\right)$ attains its unique minimum when $\|p_{ij}\|$ takes the value of the desired distance.

One example of such potential functions is as follows [42]:

$$
\psi\left(\|p_{ij}\|\right) = \begin{cases} +\infty, & \|p_{ij}\| = 0 \\ \frac{r}{\|p_{ij}\|(r-\|p_{ij}\|)}, & \|p_{ij}\| \in (0, r) \\ +\infty, & \|p_{ij}\| = r \end{cases} \tag{5.5}
$$

The potential function is shown in Figure 5.1.

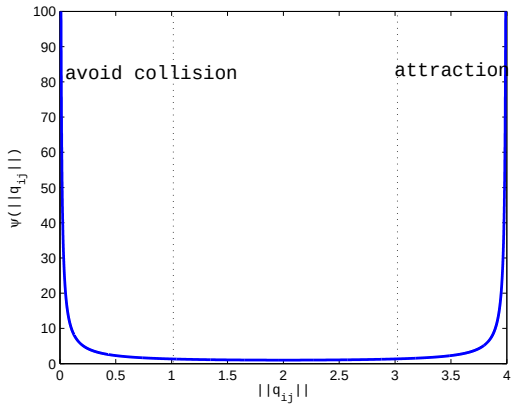

Figure 5.1: The potential function $\psi_{ij}(\|p_{ij}\|)$ with $r = 4$. The function is symmetric with respect to agents i and j. It preserves the distance $\|p_{ij}\| \to \frac{r}{2}$.

5.3.3 Control Design

The adjacency matrix $A(t) = (a_{ij}(t))$ of system in Eq. (5.1) is defined as $a_{ij}(t) = 1$ if $(i, j) \in \mathcal{E}(t)$, otherwise, $a_{ij}(t) = 0$. The Laplacian is defined as $L(t) = D(A(t)) - A(t)$, where the degree matrix $D(A(t))$ is a diagonal matrix with the ith diagonal element equal to $\sum_{j=1, j\neq i}^{N} a_{ij}(t)$. Denote $\lambda_1(\cdot)$ as the minimal eigenvalue of a symmetric matrix and the eigenvalues of $L(t)$ can be written as $\lambda_1(L(t)) \leq \ldots \leq \lambda_N(L(t))$. Then, $\lambda_1(L(t)) = 0$ and we can deduce that its corresponding eigenvector is $1 = [1, 1, \ldots, 1]^T \in R^N$. Furthermore, if G(t) is a connected graph, then $\lambda_2(L(t)) > 0$ [36]. For notational convenience, we denote

$$p = \begin{bmatrix} p_i \\ p_2 \\ \vdots \\ p_N \end{bmatrix}, \quad v = \begin{bmatrix} v_1 \\ v_2 \\ \vdots \\ v_N \end{bmatrix}.$$

Lemma 6 *[43] Suppose G is an undirected graph of order N, and let G_1 be the*

undirected graph by adding some edge(s) into the graph G. Then $\lambda_i(L_1) \geq \lambda_i(L)$, for all $i = 1, 2, \ldots, N$, where L_1 and L are the Laplacian matrices of G_1 and G, respectively.

We define the sum of the total artificial potential energy and the total relative kinetic energy among agents and center of mass as

$$\hat{V}(\hat{p}, v, p, \bar{v}) = \frac{1}{2}\sum_{i=1}^{N}(U_i(p, \bar{p})) + \frac{1}{2}\sum_{i=1}^{N}(v_i - \bar{v})^T(v_i - \bar{v}), \tag{5.6}$$

where

$$U_i(p, \bar{p}) = \sum_{j \in \mathcal{N}_i(t)} \psi(\|\hat{p}_i - \hat{p}_j\|). \tag{5.7}$$

Theorem 2 *Consider a system of N autonomous agents with dynamic motion as in (5.1) driven by the control law in (5.3). Suppose that the initial network $G(0)$ is connected, the initial energy $\hat{V}_{t_0}$ is finite, and $\rho(L(t_0)) - \ell N I > 0$. Then, the following results hold:*

(1) $G(t)$ will remain connected all the time $t \geq 0$;

(2) all agents asymptotically approach the same velocity and attain a relatively invariable distance;

(3) each agent's global potential $\sum_{j \in \mathcal{N}_i(t)} \nabla_{p_i} \psi(\|p_{ij}\|)$ is locally minimized for almost every final configuration;

(4) collisions among agents are avoided.

Proof. *We first prove part (1) of Theorem 2.* Suppose the difference of position and velocity between agent i and the center of mass are given as $\hat{p}_i = p_i - \bar{p}$ and

$\hat{v}_i = v_i - \bar{v}_i$, respectively. Simple calculations given

$$\begin{aligned}
\dot{\hat{p}}_i &= \hat{v}_i, \\
\dot{\hat{v}}_i &= f_i(v_i) - \frac{1}{N}\sum_{j=1}^{N} f_j(v_j) - \sum_{j\in\mathcal{N}_i(t)} \nabla_{\hat{p}_i}\psi(\|\hat{p}_{ij}\|) \\
&\quad -\rho \sum_{j\in\mathcal{N}_i(t)} a_{ij}\left\{ \text{sgn}\left[\sum_{k\in\mathcal{N}_i(t)} a_{ik}(\hat{v}_i - \hat{v}_k)\right] - \text{sgn}\left[\sum_{k\in\mathcal{N}_j(t)} a_{jk}(\hat{v}_j - \hat{v}_k)\right]\right\}
\end{aligned} \tag{5.8}$$

Moreover, the potential energy function in Eq. (5.3) can be rewritten as

$$V(\hat{p},\hat{v}) = \frac{1}{2}\sum_{i=1}^{N}(U_i(\hat{p}) + \hat{v}_i^T\hat{v}_i), \tag{5.9}$$

where

$$U_i(\hat{p}) = \sum_{j\in\mathcal{N}_i(t)} \psi\left(\|\hat{p}_i - \hat{p}_j\|\right), \tag{5.10}$$

and

$$\hat{p} = \begin{bmatrix} \hat{p}_1 \\ \hat{p}_2 \\ \vdots \\ \hat{p}_N \end{bmatrix}, \quad \hat{v} = \begin{bmatrix} \hat{v}_1 \\ \hat{v}_2 \\ \vdots \\ \hat{v}_N \end{bmatrix},$$

where,$\hat{v}_i = v_i - \bar{v}$, and $\hat{p}_i = p_i - \bar{p}$. $V(\hat{p},\hat{v})$ is a positive semi-definite function of $(\hat{p},\hat{v})$.

Suppose that $G(t)$ switches at time $t_k, k = 1, 2, \ldots$, and remains fixed over each time interval $[t_{k-1}, t_k]$. Without loss of generality, we assume that $t_0 = 0$ and the

initial energy $\hat{V}(t_0)$ is finite. Considering the time derivative of $Q(t)$ on $[t_0, t_1)$ gives

$$\begin{aligned}
\dot{\hat{V}} &= \sum_{i=1}^{N} \hat{v}_i^T \left[f_i(v_i) - \frac{1}{N} \sum_{i=1}^{N} f_j(v_j) \right] \\
&\quad - \sum_{i=1}^{N} \hat{v}_i^T \rho \sum_{j \in \mathcal{N}_i(t)} a_{ij} \left\{ \operatorname{sgn} \left[\sum_{k \in \mathcal{N}_i(t)} a_{ik}(\hat{v}_i - \hat{v}_k) \right] - \operatorname{sgn} \left[\sum_{k \in \mathcal{N}_j(t)} a_{jk}(\hat{v}_j - \hat{v}_k) \right] \right\} \\
&= \sum_{i=1}^{N} \hat{v}_i^T \left[f_i(v_i) - \frac{1}{N} \sum_{i=1}^{N} f_j(v_j) \right] - \rho \hat{v}^T L(t_0) \operatorname{sgn}[L(t_0)\hat{v}] \\
&\leq \|\ell I \hat{v}\|_1 - \rho \|L(t_0)\hat{v}\|_1 \\
&= (\|\ell I\|_1 - \rho \|L(t_0)\|) \|\hat{v}\|_1 \\
&\leq 0, \qquad (5.11)
\end{aligned}$$

which implies that $\hat{V}(t) < \hat{V}(t_0) < \infty, \forall t \in [t_0, t_1)$. By the definition of the potential function, $\lim_{p_{ij}(t) \to r} \psi(\|p_{ij}(t)\|) = \infty$. Therefore, there is no distance of existing edges tend to r for $t \in [t_0, t_1)$, which implies that no edge will be lost before time t_1. Thus, new edges must be added in the interaction network at switching time t_1. Note that the hysteresis ensures that if a finite number of links are added to $G(t)$, then the associated potentials remain finite. Thus, $\hat{V}(t_1)$ is finite.

From Lemma **??** and $\rho(L(t_0)) - \ell N I > 0$, we have

$$\rho(L(t_{k-1})) - \ell N I > 0.$$

Similar to the above analysis, the time derivative of $V(t)$ in every $[t_{k-1}, t_k)$ interval is

$$\begin{aligned}
\dot{\hat{V}} &= \sum_{i=1}^{N} \hat{v}_i^T \left[f_i(v_i) - \frac{1}{N} \sum_{i=1}^{N} f_j(v_j) \right] \\
&\quad - \sum_{i=1}^{N} \hat{v}_i^T \rho \sum_{j \in \mathcal{N}_i(t)} a_{ij} \left\{ \operatorname{sgn} \left[\sum_{k \in \mathcal{N}_i(t)} a_{i,k} (\hat{v}_i - \hat{v}_k) \right] - \operatorname{sgn} \left[\sum_{k \in \mathcal{N}_j(t)} a_{j,k} (\hat{v}_j - \hat{v}_k) \right] \right\} \\
&= \sum_{i=1}^{N} \hat{v}_i^T \left[f_i(v_i) - \frac{1}{N} \sum_{i=1}^{N} f_i(v_j) \right] - \rho \hat{v}^T L(t_{k-1}) \operatorname{sgn}[L(t_{k-1}) \hat{v}] \\
&\leq \|\ell I \hat{v}\|_1 - \rho \|L(t_{k-1}) \hat{v}\|_1 \\
&= (\|\ell I\|_1 - \rho \|L(t_{k-1})\|) \|\hat{v}\|_1 \\
&\leq 0, \qquad (5.12)
\end{aligned}$$

which implies that $\hat{V}(t) < \hat{V}(t_{k-1}) < \infty, \forall t \in [t_{k-1}, t_k), k = 1, 2, \ldots$. Therefore, no distance of existing edges will tend to r for $t \in [t_{k-1}, t_k)$, which also implies that no edges will be lost before time t_k and $V(t_k)$ is finite. Since $G(0)$ is connected and no edge in $E(0)$ can be lost, $G(t)$ will remain connected for all $t \geq 0$.

We now prove parts (2) and part(3) of Theorem 2. Assume that n_k new edges are added to the evolving network G at time t_k. Because $0 < n_k \leq \frac{(N-1)(N-2)}{2} \triangleq \bar{N}$ from Eq. (5.6) and Eq. (5.11), we have

$$\hat{V}(t_k) \leq \hat{V}_0 + (n_1 + n_2 + \ldots + n_k) \psi(\|r - \varepsilon\|) = \hat{V}_{\max} \qquad (5.13)$$

Due to the fact that there are at most M new edges added to $G(t)$, we know $k \leq \bar{N}$ and $V_t \leq V_{\max}$ for all $t \geq 0$. Then, the number of switching times k of system (5.1) is finite, namely, $G(t)$ finally becomes fixed. Thus, we only need to discuss the behaviors on the time interval (t_k, ∞). Since that all the lengths of edges are no

longer than $\psi^{-1}(\hat{V}_{\max})$, then the set

$$\Omega = \left\{ \widehat{\tilde{p}} \in \mathcal{G}, \tilde{v} \in R_{Nn} \middle| \hat{V}(\widehat{\tilde{p}}, \hat{v}) \leq \hat{V}_{\max} \right\} \tag{5.14}$$

is positively invariant, where

$$\mathcal{G} = \left\{ \widehat{\tilde{p}} \in R^{N^2 n} \middle| \|p_{ij}\| \in [0, \psi^{-1}(\hat{V}_{\max})], \forall (i,j) \in \mathcal{E}(t) \right\}$$

and $\widehat{\tilde{p}} = [p_{11}^T, p_{12}^T, \ldots, p_{1N}^T, \ldots, p_{N1}^T, p_{N2}^T, \ldots p_{NN}^T]$.

Since $G(t)$ is connected for all $t \geq 0$ as mentioned above, for all i and j we have $\|\hat{p}_i\| - \|\hat{p}_j\| < (N-1)$. Due to the fact that $\hat{V}(t) \leq \hat{V}_{\max}$, we have $\hat{v}_i^T \hat{v}_i < 2\hat{V}_{\max}$, and so $\|\hat{v}_i\| \leq \sqrt{2\hat{V}_{\max}}$. Therefore, the set Ω satisfying $\hat{V}_t \leq \hat{V}_{\max}$ is closed, and furthermore, compact. As we know, system in Eq. (5.1) with control input in Eq. (5.3) is autonomous on the concerned time interval (t_k, ∞). Hence, the LaSalle Invariance Principle can be applied to conclude that if we limit the initial conditions of the system to be in Ω, then the corresponding trajectories will converge to the largest invariant set inside the region

$$\Gamma = \left\{ \widehat{\tilde{p}} \in \mathcal{G}, \hat{v} \in R_{Nn} \middle| \dot{\hat{V}} = 0 \right\}.$$

From (5.12), $\dot{\hat{V}} = 0$ if and only if $\hat{v}_1 = \ldots = \hat{v}_N$, namely, the velocities of all agents converge to the virtual leader's velocity in an asymptotical way.

Since $\hat{v}_1 = \ldots = \hat{v}_N$, one has

$$\dot{\hat{v}}_i = -\sum_{j \in \mathcal{N}_i(t)} \frac{\partial \psi(\|p_{ij}\|)}{\partial \|p_{ij}\|} \frac{1}{\|p_{ij}\|} (p_i - p_j) = 0 \tag{5.15}$$

for all $i = 1, 2, \ldots, N$.

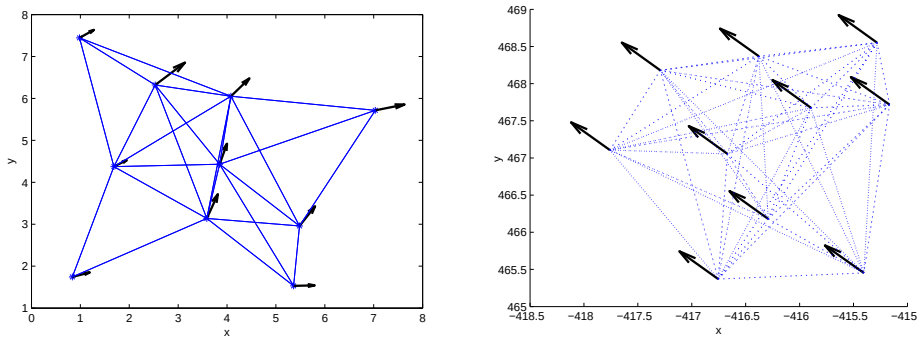

Figure 5.2: Initial and final states of multiple agents ($n = 10$) with velocity vectors. (a) the Initial states; and (b) the finial states.

Generally, every final configuration will locally minimize each agent's global potential, unless the initial configuration of the agents is close enough to the global minimum.

We now prove part (4) of of Theorem 2. From (5.14), $\hat{V}(\widehat{\tilde{p}}, \hat{v}) \leq \hat{V}_{\max}$ for all $t \geq 0$. However, we have $\lim_{\|p_{ij}(t)\| \to r} \psi(\|p_{ij}(t)\|) = \infty$ from the definition of potential functions. Hence, collisions among agents can be avoided.

□

5.4 Simulation Results

Consider a multi-agent system under the control protocol in Eq. (5.3) with 10 agents in a two-dimensional Euclidean space. For simplicity of presentation, the intrinsic dynamic of each agent is governed by $f_i(v_i) = [3\cos(i \cdot v_{i1} + v_{i2}), 3\sin(v_{i1} + i \cdot v_{i2})]^T, i = 1, 2, \ldots, 10$. The potential function is designed as in Eq. (5.6) with the influencing/sensing radius $r = 4$ and $\varepsilon = 0.1$. Initial positions and initial velocities of agents are chosen randomly from the plane $[0, 8] \times [0, 8]$ and $[0, 3] \times [0, 3]$ shown in Figure 5.2(a), the dotted lines represent the neighboring relations, and the solid lines with arrows represent the velocity vectors. We choose $\rho = 10$. Then the

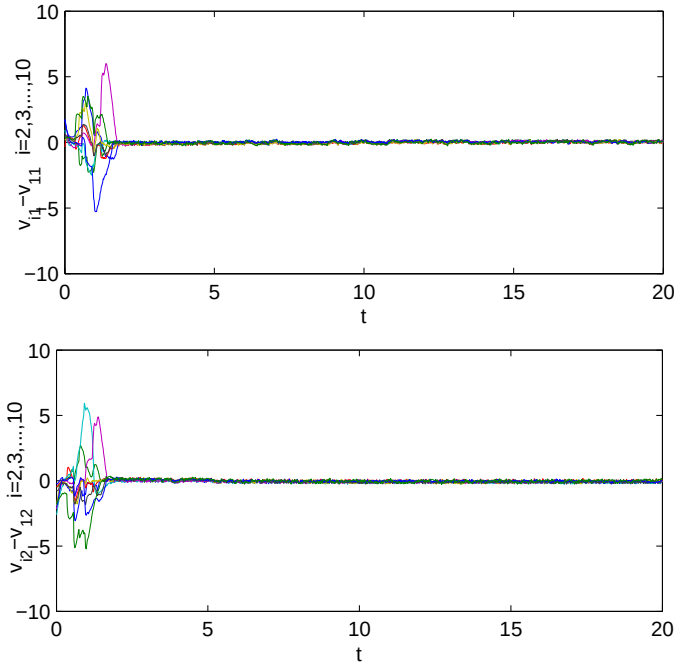

Figure 5.3: Relative velocity states between agent 1 and agent $i, (i = 2, 3, \ldots, 10)$.

multiple autonomous agents move with the same velocity as shown in Figure 5.2(b), from $t = 0s$ to $t = 20s$. The relative velocity values between agent 1 and agent $i, (i = 2, 3, \ldots, 10)$ are shown in Figure 5.3.

5.5 Conclusion

In summary, we have investigated a multi-agent flocking problem, where each agent has heterogeneous nonlinear dynamics. An artificial potential function and connectivity-preserving algorithm have been proposed to guarantee not to lose the existing edges, which shows that all agents can move with the same velocity and preserving the network connectivity without collision. From the numerical examples, the theoretical results are verified effectively.

6. SUMMARY AND FUTURE RESEARCH

6.1 Contributions

In this thesis, I have considered four problems on the modeling and control of multi-agent systems as shown in Figure 1.2. I have designed the modeling rules and control approaches to these problems. Numerical examples and theoretical proofs have also been presented. I summarize the contributions of this thesis as follows:

1) I have proposed an improved adaptive-velocity self-organizing model as a prospective candidate in order to enhance high-speed convergence and accelerate convergence. Moreover, a new way to assign weights has been proposed to reinforce convergence under very high-speed conditions. This innovative result has been organized into a scientific paper and submitted to *Physica D*.

2) To the best of my knowledge, input saturation has not been taken into account in the output regulation problem for general dynamic agents. In this thesis, I have solved this problem via low gain feedback such that the tracking error can be eliminated with bounded control inputs.

3) I have investigated the multi-agent flocking problem with heterogeneous nonlinear dynamics. I constructed a potential function and a connectivity-preserving flocking algorithm to ensure the agents stay connected. The mild assumption is made that the initial network is connected, and the coupling strength of the initial network of the nonlinear velocity consensus term is greater than a threshold. This innovative result has been published as a scientific paper in *Neurocomputing*.

6.2 Future Research

There are many promising directions for future research and applications. Here, I outline several potential extensions.

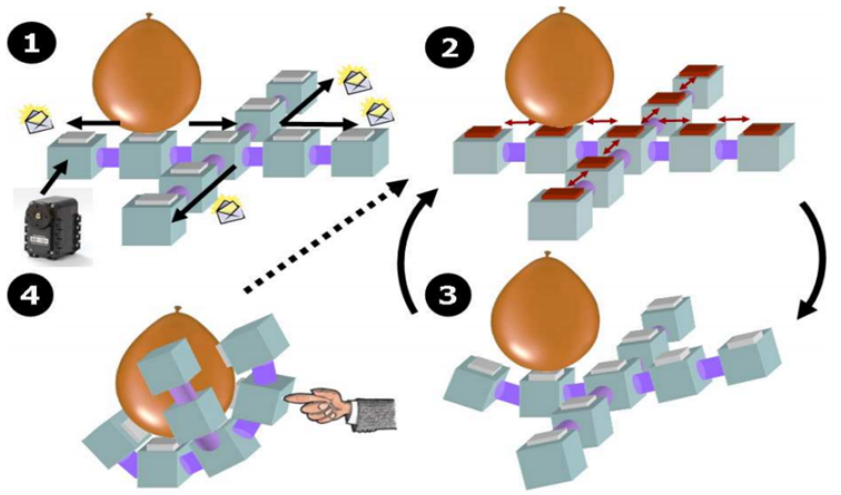

Figure 6.1: Algorithmic overview of the grasping task. [44] Step 1: The first module starts sensing the presence of the object. It starts sending messages to it neighbors. Steps 2 and 3: Agents perform iterative sensing and actuation until they converge to the desired state. Step 4: When the system is perturbed, it goes back to Step 2.

6.2.1 Deconstruction and Distributed Control of Complex Robotic Systems

It is known that in complex-structural and/or multi-task systems, centralized controllers are difficult to design, despite the delay and asynchronization between components caused by computational complexity. However, even though they seem atypical multi-agent systems, it is possible for us to decompose the complex systems into several functional and/or structural parts. Therefore, decentralized controllers can be developed independently for these single-functional or simple-structural part-s and then designed to interact with each other to achieve the overall objective. Although, in the current stage, decentralized control still has many constraints and unsolved problems, I believe the idea of decentralized control-design from the bottom up-will be developed and applied widely in the near future.

As an example, Figure 6.1 shows a robot 'hand' controlled by distributed con-trollers [44].

6.2.2 Control of Multi-Agent Formation and Applications

Based on the linear multi-agent model, we have found that there exists a relationship between the final stable formation and the eigenvector corresponding to the '0 eigenvalue of the closed-loop system matrix A. We have proved that the consensus problem can be treated as a special case in which the entries of the eigenvector corresponding to the '0 eigenvalue are uniform. But what is the sufficient condition for a multi-agent system to achieve a specific formation? We could further work on the problem to generalize a criterion for achieving any desired formation.

REFERENCES

[1] Shaw E. Fish in schools. Natural History, 1975, 84(8): 4045.

[2] Vicsek T. A question of scale. Nature, 2001, 411: 421421.

[3] Flierl G, Grunbaum D, Levin S, Olson D. From individuals to aggregations: the interplay between behavior and physics. Journal of Theoretical Biology, 1999, 196: 397454.

[4] Partridge B L. The chorus-line hypothesis of maneuver in avian flocks. Nature, 1984, 309: 344345.

[5] Dong, H., Zhao, Y., Gao, S. A fuzzy-rule-based Couzin model. Journal of Control Theory and Applications, 2013, 11(2): 311-315.

[6] Couzin I D, Krause J, Franks N R, et al. Effective leadership and decision-making in animal groups on the move. Nature, 2005, 433(7025): 513-516.

[7] Reynolds C W. Flocks, herds and schools: A distributed behavioral model. ACM Siggraph Computer Graphics, 1987, 21(4): 25-34.

[8] Vicsek T, Czirók A, Ben-Jacob E, et al. Novel type of phase transition in a system of self-driven particles. Physical Review Letters, 1995, 75(6): 1226.

[9] Couzin I D, Krause J, James R, Ruxton G D, Franks N R. Collective memory and spatial sorting in animal groups. Journal of Theoretical Biology, 2002, 218(1): 1-11.

[10] Li W and Wang X, Adaptive velocity strategy for swarm aggregation. Physcal Review E, 2012, 75: 201917.

[11] Dong H, Zhao Y, Wu J, et al. A velocity-adaptive Couzin model and its performance. Physica A: Statistical Mechanics and its Applications, 2012, 391(5): 2145-2153.

[12] Gao J, Chen Z, Cai Y, et al. Enhancing the convergence efficiency of a self-propelled agent system via a weighted model. Physical Review E, 2010, 81(4): 041918.

[13] Wang X F. Complex networks: topology, dynamics and synchronization. International Journal of Bifurcation and Chaos, 2002, 12(05): 885-916.

[14] Olfati-Saber R, Murray R M. Consensus problems in networks of agents with switching topology and time-delays. Automatic Control, IEEE Transactions on, 2004, 49(9): 1520-1533.

[15] Liu X, Lin H, Chen B M. Graph-theoretic characterisations of structural controllability for multi-agent system with switching topology. International Journal of Control, 2013, 86(2): 222-231.

[16] Olfati-Saber R, Fax J A, Murray R M. Consensus and cooperation in networked multi-agent systems. Proceedings of the IEEE, 2007, 95(1): 215233.

[17] Zhang H, Lewis F L, Das A. Optimal design for synchronization of cooperative systems: state feedback, observer and output feedback. Automatic Control, IEEE Transactions on, 2011, 56(8): 1948-1952.

[18] Ni W, Cheng D. Leader-following consensus of multi-agent systems under fixed and switching topologies. Systems & Control Letters, 2010, 59(3): 209-217.

[19] Ren W. Consensus tracking under directed interaction topologies: Algorithms and experiments. American Control Conference, 2008, IEEE, 2008: 742-747.

[20] Hong Y, Hu J, Gao L. Tracking control for multi-agent consensus with an active leader and variable topology. Automatica, 2006, 42(7): 1177-1182.

[21] Ihle I A F, Jouffroy J, Fossen T I. Robust formation control of marine craft using lagrange multipliers. Group coordination and cooperative control, Springer Berlin Heidelberg, 2006: 113-129.

[22] Liu X, Output regulation of strongly coupled symmetric composite systems. Automatica, 1992, 28(5): 1037-1041.

[23] Tarbouriech S, Garcia G, Gomes da Silva Jr. J M, Queinnec I. Stability and Stabilization of Linear Systems with Saturating Actuators. Springer-Verlag, 2011.

[24] Kapila V, Grigoriadis K. Actuator Saturation Control. New York, 2002.

[25] Kapoor N, Teel A R, Daoutidis P. An anti-windup design for linear systems with input saturation. Automatica, 1998, 34(5): 559574.

[26] Lin Z. Low gain feedback. London: springer, 1999.

[27] Jadbabaie A, Lin J, Morse A, Coordination of groups of mobile autonomous agents using nearest neighbor rules, Automatic Control, IEEE Transactions on, 2003, 48: 9881001.

[28] Su H, Wang X, Lin Z, Synchronization of coupled harmonic oscillators in a dynamic proximity network. Automatica, 2009, 45: 22862291.

[29] Su H, Chen G, Wang X, Lin Z, Adaptive second-order consensus of networked mobile agents with nonlinear dynamics. Automatica, 2011, 47: 368375.

[30] Abdessameud A, Tayebi A. Motion Coordination for VTOL Unmanned Aerial Vehicles: Attitude Synchronization and Formation Control. Springer, 2013.

[31] Shi H, Wang L, Chu T G. Virtual leader approach to coordinated control of multiple mobile agents with asymmetric interactions. Physica D, 2006, 213: 5165.

[32] Olfati-Saber R. Flocking for multi-agent dynamic systems: Algorithms and theory. Automatic Control, IEEE Transactions on, 2006, 51(3): 401420.

[33] Su H, Wang X, Lin Z. Flocking of multi-agents with a virtual leader, part I: with minority of informed agents. In Proceedings of the IEEE Conference on Decision and Control, 2007: 2937-2942.

[34] Toner J, Tu Y. Flocks, herds, and schools: a quantitative theory of flocking. Physical Review E, 1998,58(4): 4828-4858.

[35] Mogilner A, Edelstein-keshet L. A nonlocal model for a swarm. Journal of Mathematical Biology. 1999, 38: 534-570.

[36] Godsil C, Royle G, Godsil C D. Algebraic graph theory. New York: Springer, 2001.

[37] Lewis F, Zhang H, Hengster-Movric K, et al. Cooperative control of multi-agent systems: optimal and adaptive design approaches. Springer Science & Business Media, 2013.

[38] Beard R, McLain T, Nelson D, Kingston D, Johanson D. Decentralized cooperative aerial surveillance using fixed-wing miniature UAVs. Proceedings of the IEEE, 2006, 94(7): 13061324.

[39] Bhattacharyya S P, Datta A, Keel L H. Linear control theory: structure, robustness, and optimization. CRC press, 2010.

[40] Su Y, Huang J. Cooperative output regulation of linear multi-agent systems. Automatic Control, IEEE Transactions on, 2012, 57(4): 1062-1066.

[41] Su H, Chen M Z, Lam J, et al. Semi-global leader-following consensus of linear multi-agent systems with input saturation via low gain feedback. Circuits and Systems I: Regular Papers, IEEE Transactions on, 2013, 60(7): 1881-1889.

[42] Su H, Wang X, Chen G. Rendezvous of multiple mobile agents with preserved network connectivity. Systems & Control Letters, 2010, 59(5): 313-322.

[43] Merris R. Laplacian matrices of graphs: a survey. Linear algebra and its applications, 1994, 197: 143-176.

[44] Yu C, Biologically-inspired control for self-adaptive multi-agent systems. 2010, PhD thesis.